AD 210651

CARNEGIE INSTITUTE OF TECHNOLOGY
DEPARTMENT OF PHYSICS
Pittsburgh 13, Pennsylvania

THE TWO HALL EFFECTS OF IRON-COBALT ALLOYS

by

Frank P. Bailey, Jr.

and

SUMMARY OF RESEARCH

by

Emerson M. Pugh

FINAL REPORT

OFFICE OF NAVAL RESEARCH

CONTRACT Nonr - 266(04)

December 31, 1958

Carnegie Institute of Technology
Department of Physics
Contract Nonr-760(04)
Office of Naval Research

FINAL REPORT

THE TWO HALL EFFECTS OF IRON-COBALT ALLOYS

By Frank P. Beitel, Jr.

and

SUMMARY OF RESEARCH DONE UNDER
CONTRACTS Nonr-206(00)
760(04)

By Emerson M. Pugh

December 31, 1958

TABLE OF CONTENTS

LIST OF FIGURES

LIST OF FIGURES (Cont'd)

LIST OF TABLES

ABSTRACT

The Hall coefficients and resistivities of the Fe-Co alloys ~~have been~~ were measured at 77°K, 169°K, and room temperature using fields up to 3.3 weber/m^2. For less than 0.2°/o Co in Fe the ordinary Hall coefficient R_o^* is positive at room temperature and negative at low temperatures; for all other compositions R_o^* is negative. Analysis with a simple band model shows that, as iron is added to cobalt, one half of the 3d band remains filled for up to 20°/o Fe. It then empties, having about 0.2 holes per atom at 50°/o Fe. At 65°/o Fe the bands apparently shift so that again one 3d sub-band is filled. The extraordinary Hall coefficient R_1^* is positive for less than 25°/o Co in Fe, but for all other compositions it changes from positive to negative as the temperature decreases from 300°K to 169°K. R_1^* and the resistivity ρ are related by $R_1^* = a + b\rho^2$. The influence of the approach to magnetic saturation on the Hall curves is examined in detail. The Hall effect is not very useful for studying the approach to saturation, but magnetic data can be used to calculate corrections to R_o^* and R_1^*.

Based on a thesis submitted by Frank P. Beitel, Jr. to the Carnegie Institute of Technology in partial fulfillment of the requirements for the degree of Doctor of Philosophy.

1. INTRODUCTION

If a magnetic field is applied perpendicular to an electric current in a material, then an electric field is produced perpendicular to both the current and the magnetic field. This phenomenon is called the Hall effect, for it was first observed by E. H. Hall in 1879. Early experimental studies on many materials showed that the Hall electric field E_H was proportional to both the current density j and the magnetic induction B; that is,

$$E_H = RjB \qquad (1.1)$$

where R was called the Hall coefficient. For ferromagnetic materials, however, the proportionality to B did not hold at higher fields, but the deviation was generally noted and then ignored. Kundt[1] first pointed out that, at low fields, E_H was proportional to M rather than B or H. In 1929 Smith and Sears[2] split their data on permalloy into two parts, one part proportional to M and the other proportional to H. Shortly thereafter Pugh[3] observed that the Hall emf V ($V = wE_H$, where w is the sample width) followed a hysteresis curve. On the basis of this work and the results of Smith and Sears he proposed that $E_H/j = V/wj = Vt/I$, should be written as the sum of a term

---

1/ A. Kundt, Wied. Ann. 49, 257 (1893).

2/ A. W. Smith and R. W. Sears, Phys. Rev. 34, 1466 (1929).

3/ E. M. Pugh, Phys. Rev. 36, 1503 (1930).

proportional to H and a term proportional to M; or, in the usual form,

$$Vt/I = R_o(\mu_o H) + R_1 M = R_o B + (R_1 - R_o)M \qquad (1.2)$$

where I is the sample current and t is the sample thickness. Since early measurements were made at relatively low fields, the second term was observed but the first was not.

Simple arguments using the Lorentz force on a moving charged particle gave a simple expression for the Hall coefficient R in Eq. (1.1); and the Sommerfeld[4] free electron model of a metal gave the same result, namely

$$R = -1/Nne \qquad (1.3)$$

where

N = number of atoms per m^3,

n = number of conduction electrons per atom,

and e = $+1.6 \times 10^{-19}$ coul = magnitude of the electronic charge.

Early measurements of the Hall effect gave reasonable values for n in most cases, but in ferromagnetic materials the values were much too small. On the basis of a reexamination of early data for nickel[5], it was proposed[6] that the R of Eq. (1.3) should be identified with the R_o of Eq. (1.2). Thus, R_o was called the

---

4/ A. Sommerfeld and N. H. Frank, Rev. Mod. Phys. 3, 1 (1931).

5/ A. W. Smith, Phys. Rev. 30, 1 (1910).

6/ E. M. Pugh, N. Rostoker, and A. I. Schindler, Phys. Rev. 80, 688 (1950).

ordinary coefficient and R_1 was called the extraordinary coefficient. The Hall effects were measured in the Cu-Ni alloys by Schindler[7] and Cohen[8] and in the Co-Ni alloys by Foner[9]. Analyzing their data on the basis of the relation

$$R_o = -1/Nne \qquad (1.4)$$

they found that the effective number of conduction electrons per atom, n^*, differed by less than a factor of 2 from the number of 4s electrons determined from magnetic data.

Pugh[10] explained both the factor of 2 disagreement between n^* and n_s and the temperature dependence of the Cu-Ni alloys with a model in which the 4s band was split into two sub-bands with electron spins aligned parallel and anti-parallel, respectively, to the magnetic field. The mobilities of the electrons in the two bands were not the same, due to the difference in the probabilities of being scattered into the 3d band, so that the sub-bands contributed differently to the conduction even though they contained the same number of electrons. Allison and Pugh[11] studied three Cu-Ni alloys more completely from 4^oK to well above their Curie temperatures. They found good agreement

---

7/ A. I. Schindler and E. M. Pugh, Phys. Rev. 89, 295 (1953).

8/ P. Cohen Thesis, Navy Contract Nonr-760(04) Technical Rpt. No. 1, June 1955.

9/ S. Foner and E. M. Pugh, Phys. Rev. 91, 20 (1953).

10/ E. M. Pugh, Phys. Rev. 97, 647 (1955).

11/ F. E. Allison and E. M. Pugh, Phys. Rev. 102, 1281 (1956).

between the temperature dependence observed and that predicted by the above band model with the additional assumption that one 3d sub-band was completely filled at absolute zero.

Thus, it has been shown that R_o is closely related to the number of conduction electrons per atom, and a simple band model has proved to be quite successful in explaining the dependence of the ordinary Hall coefficients of the 3d-4s transition alloys upon both composition and temperature.

The origin of the extraordinary Hall coefficient R_1 is more obscure and was at first attributed to the existence of an effective field such that

$$\mu_o H_{eff} = \mu_o H + \alpha M$$

where α was called the field parameter. The Hall electric field per unit current density was then written in the form

$$\begin{aligned} Vt/I &= R_o \mu_o H_{eff} \\ &= R_o \mu_o H + R_o \alpha M. \end{aligned}$$

Thus, from Eq. (1.2), $R_1 = \alpha R_o$. Pugh and Rostoker[12] discussed various proposals which had been made concerning the origin of the effective field and concluded that only the spin-orbit coupling of the conduction electrons offered a possible explanation. In 1954, Karplus and Luttinger[13] succeeded in explaining the

---

12/ E. M. Pugh and N. Rostoker, Rev. Mod. Phys. 25, 151 (1953).

13/ R. Karplus and J. M. Luttinger, Phys. Rev. 95, 1154 (1954).

extraordinary effect on the basis of spin-orbit coupling and found that $R_1 = A\rho^2$, where ρ is the resistivity. A theory of the spin-orbit interaction in an alternating electric field which was developed shortly thereafter[14] gave the same result in the limit of a static electric field. Smit[15,16] also considered the spin-orbit interaction and concluded that $(R_1 - R_o)$ should be proportional to ρ^2. A number of investigators have found that for various materials $R_1 = A\rho^n$ where $n \cong 2$, while Smit[15] has found a similar result for $R_1 - R_o$.

For alloys with effective atomic numbers less than that of cobalt (that is, alloys of Fe-Co, Fe-Mn, etc.), the electronic configurations are not as well known as are those for the Cu-Ni and Ni-Co alloys. While one 3d sub-band is filled in the Cu-Ni and Ni-Co alloys, it is believed that holes begin to appear in both 3d sub-bands as iron is added to cobalt[17]. Measurements of the two Hall effects have been made for a series of Fe-Co alloys; and the major part of this thesis concerns the measurement of R_o, which should give more information about their electronic configurations. The resistivities of the alloys also were measured in order that the relation between R_1 and ρ could be examined.

14/ P. N. Argyres, Phys. Rev. 97, 334 (1955).

15/ J. Smit, Physica 21, 877 (1955).

16/ J. Smit, Physica 24, 39 (1958).

17/ B. R. Coles and W. R. Bitler, Phil. Mag. 1, 477 (1956).

Foner[18] observed that in Armco iron saturation in the Hall effect was not reached for fields below 2.6 weber/m^2, and he suggested that Hall data could be used in studying magnetic properties at high fields. Since the Fe-Co alloys all have very high values for M_s, difficulty in determining R_o and R_1 accurately was anticipated due to the contribution of a $\partial M/\partial B$ term to the slope of the Hall emf curve at high fields. Accordingly, the approach to magnetic saturation and its effect on measurements of R_o and R_1 is considered in detail in this thesis.

18/ S. Foner, Phys. Rev. 101, 1648 (1956).

ACKNOWLEDGMENTS

I am most grateful to Professor Emerson M. Pugh for suggesting this problem and for his sincere encouragement and guidance throughout the course of the work.

I am also grateful to the various members of the Department of Physics and Metallurgy who have contributed advice and discussion, particularly to Dr. F. E. Allison and Mr. J. A. Dreesen.

I wish to thank the low temperature group and the X-ray group for the use of their facilities and the machine shop personnel for their kind cooperation.

Finally I am indebted to the Office of Naval Research for supporting the research, to Carnegie Institute of Technology for several scholarship awards, and to Westinghouse Electric Corporation and Allegheny Ludlum Steel Corporation for furnishing sample materials.

2. UNITS

The two Hall coefficients are usually expressed in terms of the unit 10^{-13} volt-cm/amp-gauss which is a mixture of Gaussian and practical units. This is a natural unit; for the combination of terms results directly from the method of measurement, and one conduction electron per atom gives values of the order of 10 units for R_o.

The conversion to the practical system of units is quite simple; the pertinent equations are changed slightly, and the troublesome factors c and 4π are eliminated. In this system the relation between B, H, and M can be written as

$$B = \mu_o H + M$$

where the units of B, $\mu_o H$, and M are weber/m^2. Consequently, if R_o is defined sc that it corresponds to the usual definition of the ordinary Hall coefficient, the quantities μ_o and H appear only as the product $\mu_o H$ and the Hall equation may be written[19/]

$$Vt/I = R_o(\mu_o H) + R_1 M \qquad (1.2)$$
$$= R_o B + (R_1 - R_o)M.$$

The result of the simplest theory of the Hall effect expressed in the practical system of units is

$$R_o = -1/Nne \qquad (1.4)$$

where N is the number of atoms per m^3, n is the number of

19/ Some authors have defines R_1 through the term $R_1 M$ while others have used $R_1 4\pi M$, where M has the same meaning in the Gaussian system in both cases. R_1 as defined here corresponds to the latter case.

conduction electrons per atom, and e is $+1.6 \times 10^{-19}$ coulomb, the magnitude of the electronic charge. Thus, the units of R_o and R_1 are simply m^3/coulomb; and, from the definitions of the units, 1 m^3/coul = 1 v-m^3/amp-weber, whence

$$10^{-13} \text{ v-cm/amp-gauss} = 10^{-11} \text{ v-m}^3\text{/amp-weber}$$
$$= 10^{-11} \text{ m}^3\text{/coul}.$$

Throughout this thesis, except for a few cases in which different units are specifically noted, equations are written in the practical system; B, $\mu_o H$, and M are expressed in weber/m^2; and R_o and R_1 are expressed in terms of 10^{-11} m^3/coul. R_o and R_1, therefore, may be compared directly with values stated in terms of 10^{-13} v-cm/amp-gauss since the two units are identical, provided of course that the definitions of R_1 do not differ by the factor 4π.

3. THEORY

A. Ordinary Hall Effect

Since the theory of the ordinary Hall effect can be readily found in rather complete treatments of the transport phenomena in metals[20], it will only be outlined here to emphasize the "practical" aspects.

20/ See, for example, A. H. Wilson, The Theory of Metals (University Press, Cambridge, 1953).

The simple relation for the ordinary Hall coefficient, Eq. (1.4), can be derived directly from the expression for the Lorentz force on a moving charged particle, and this "model" provides a method for determining the sign of the Hall coefficient. Applying Fermi-Dirac statistics to the free electron model of a metal, Sommerfeld[4] succeeded in deriving the same expression.

A better description of a metal is that the electrons move about in a periodic potential due to the ion lattice rather than in a uniform potential. Such a model leads to bands of allowed electronic energies which may be separated or which may overlap. The latter situation occurs in the transition elements in which the overlapping bands have unoccupied energy levels so that electrons in both bands contribute to conduction and related phenomena. Sondheimer[21] derived an expression for the Hall coefficient of metals with two overlapping bands by solving the Boltzmann transport equation under the assumptions that (1) there was hole conduction in one band (3d band) and electronic conduction in the other (4s band), (2) the bands were parabolic bands of the standard form, and (3) the time rate of change of the distribution function due to collisions was $(\partial f/\partial t)_{coll} = -(f - f_o)/\tau$, where f_o is the distribution

---

21/ E. H. Sondheimer, Proc. Roy. Soc. (London) A193, 484 (1948).

function in the absence of applied fields and τ is a relaxation time depending only upon the energy. His result was

$$R_o = -\frac{1}{Ne}\left[\frac{1}{n_s}\left(\frac{\sigma_s}{\sigma}\right)^2 - \frac{1}{n_d}\left(\frac{\sigma_d}{\sigma}\right)^2\right]$$

where n_s and n_d are the numbers of 4s electrons and 3d holes, respectively, and σ_s and σ_d are the respective conductivities.

Pugh generalized the above result to four bands by splitting each band, 3d and 4s, into two sub-bands, each sub-band containing electrons with their magnetic moments aligned parallel to the magnetic field for one sub-band and antiparallel for the other. For this model the ordinary Hall coefficient is given by

$$R_o = -\frac{1}{Ne}\left[\frac{2}{n_s}\left(\frac{\sigma_{sa}}{\sigma}\right)^2 + \frac{2}{n_s}\left(\frac{\sigma_{sp}}{\sigma}\right)^2 - \frac{1}{n_{da}}\left(\frac{\sigma_{da}}{\sigma}\right)^2 - \frac{1}{n_{dp}}\left(\frac{\sigma_{dp}}{\sigma}\right)^2\right] \tag{3.1}$$

where the subscripts a and p refer to antiparallel and parallel alignment of the magnetic moments, respectively, and where the assumption $n_{sa} = n_{sp} = n_s/2$ has been used.

In this band model, the larger the absolute value of R_o, the fewer are the possible explanations, while the number of possible ways of explaining R_o increases tremendously as its magnitude decreases. If, for example, the antiparallel 3d band completely dominated the others, R_o would be the simple Hall coefficient $(1/Nn_{da}e)$ of the predominant band. If any one of

the other three bands increased in importance, the magnitude of R_o would decrease from its original value, whether the conduction in the second band was by holes or by electrons. Finally, as the second band became the dominant contributor to conduction, R_o would approach the simple Hall coefficient of the second band. Thus, the Hall coefficient given by Eq. (3.1) cannot exceed the simple Hall coefficient (1/Nne) of the band having the smallest number of positive carriers and cannot be (algebraically) less than the simple Hall coefficient of the band with the smallest number of negative carriers. In fact, the only way R_o can approach one of these limiting values is for the corresponding band to completely dominate the others. On the other hand, values of R_o between the two extreme values can be obtained with many combinations of the conductivities.

In the special case in which only two bands conduct and their carriers have the same sign, the maximum value of $|R_o|$ obtainable from Eq. (3.1) by changing mobilities is, as before, 1/Nqe, where q is the smaller of n_1 and n_2, and the minimum value is $1/Ne(n_1 + n_2)$. Values of R_o such that $1/Nre < |R_o| \leqq 1/Nqe$, where r is the larger of n_1 and n_2, can be obtained in only one way; but for $1/Ne(n_1 + n_2) < |R_o| \leqq 1/Nre$, R_o can be obtained for two combinations of the mobilities. The minimum value of $|R_o|$ is obtained when the mibilities of the two carriers are equal.

If 3d band conduction is neglected, Eq. (3.1) reduces to

$$R_o = -(2/Nn_s e)\left[1 - 2\beta/(1+\beta)^2\right] \qquad (3.2)$$

where $\beta = \sigma_a/\sigma_p$. On the basis of the following assumptions by Mott[22], the quantity β is given by

$$\beta = \sigma_a/\sigma_p = (N_p/N_a)^{1/3} \quad , \qquad (3.3)$$

where N_p and N_a are the numbers of holes in the parallel and antiparallel 3d sub-bands:

(1) $\sigma_a/\sigma_p = P_p/P_a$, where P_p is the probability of scattering an electron from the parallel 4s band into the parallel 3d band, and P_a is similarly defined for the antiparallel 3d band,

(2) $P_i \sim n(E_i)$, where $n(E)$ is the density of states of each 3d sub-band, and

(3) $n(E) = AE^{1/2}$, where E is measured from the top of the 3d sub-band.

The Eq. (3.2), with the auxiliary relation Eq. (3.3), has proved quite useful in the analysis of Hall data. If R_o^* is the experimental value of the ordinary Hall coefficient and if n^* is defined by $R_o^* = -1/Nn^*e$, R_o^* may be equated to R_o in Eq. (3.2) to give

$$1/n^* = (2/n_s)\left[1 - 2\beta/(1+\beta)^2\right] \qquad (3.4)$$

For an alloy in the 3d-4s transition series the quantities N_a, N_p, n_s, and the effective atomic number Z must satisfy the relations

$$N_p = (n_s/2) - Q \qquad (3.5)$$

22/ N. F. Mott, Proc. Roy. Soc. (London) A153, 699 (1936).

and $Q = [(N_a - N_p) - (28 - Z)]/2.$ (3.6)

Using Eq. (3.3), N_p may be expressed in the form

$$N_p = \beta^3(N_a - N_p)/(1 - \beta^3), \quad (3.7)$$

so that substitution into Eq. (3.5) gives

$$n_s/2 = Q + \beta^3(N_a - N_p)/(1 - \beta^3). \quad (3.8)$$

From Eq. (3.4)

$$n_s/2 = n^* (1 + \beta^2)/(1 + \beta)^2. \quad (3.9)$$

If now $g(\beta)$ is defined by

$$g(\beta) = Q + \beta^3(N_a - N_p)/(1 - \beta^3) - n^*(1 + \beta^2)/(1 + \beta)^2 \quad (3.10)$$

obviously $g(\beta) = 0$ when the values of $n_s/2$ calculated by Eqs. (3.8) and (3.9) are equal. If n^* is known from measurements of the Hall effect and if $(N_a - N_p)$ is obtained from the magnetic moment per atom, then Q can be calculated from Eq. (3.6); and Eq. (3.10) can be easily solved graphically for the value of β for which $g = 0$. In the region of interest, $0 \leqq \beta < 1$, the function $g(\beta)$ is monotonic and, therefore, has only one root. The value of β obtained from the solution $g(\beta) = 0$ can be substituted into Eq. (3.7) to give a value for N_p, from which n_s, N_a, and $N_d = N_a + N_p$ follow. The special case $\beta = 1$ occurs only when $N_a = N_p$; that is, when the 3d sub-bands are filled to the same level.

Several features of the two band model described above are useful in analyzing Hall data:

(1) On the basis of the atomic number Z and the magnetic moment per atom, the minimum possible value of n_s is 2Q, which corresponds to one 3d sub-band being filled. In this case $N_p = \beta = 0$.

(2) On the basis of Hall data, the minimum value of n_s is n^*, with the 3d sub-bands equally filled; and the maximum value of n_s is $2n^*$, with one 3d sub-band filled.

B. Associated Effects

In addition to the Hall effect there are three other so-called transverse galvano- and thermo-magnetic effects. If the application of a magnetic field perpendicular to an electric current in a material produces an electric field perpendicular to both the magnetic field and primary current, the phenomenon is called the Hall effect. If a transverse thermal gradient is produced rather than an electric field, this is called the Ettingshausen effect. The two are called galvanomagnetic effects. The corresponding thermomagnetic effects (that is, the primary current is thermal rather than electric) are called the Nernst and Righi-Leduc effects, respectively. Each of the four effects exhibits the same type dependence on H and M, requiring expression in terms of an ordinary and an extraordinary coefficient[23,24].

Allison and Pugh[11] have pointed out that the unequal heating of the two ends of a Hall sample due to the Peltier effect very often produces a primary thermal current. Obviously this can produce a spurious transverse potential due to the Nernst effect. In addition, since a potential probe of some

---

23/ E. H. Butler and E. M. Pugh, Phys. Rev. 57, 916 (1940).

24/ N. M. Genkin and G. P. Priporawa, J. Exptl. Theoret. Phys. (USSR) 26, 323 (1954).

kind must be placed on each side of the sample, the junctions between the probes and the sample could act as a differential thermocouple and introduce another spurious potential due to the thermal gradient resulting from the Ettingshausen or Righi-Leduc effects.

Methods of taking the associated effects into account have been described by several investigators. Schindler[7] and Foner[9] actually measured the latter two effects by observing the temperature of the probe-to-sample junctions with auxiliary thermocouples and converting these to potential differences with the thermocouple data for the probe and sample materials. The corrections to the Hall potentials were generally about 1%. Cohen[8] and Allison[11] used probes and wires made from the same material as the sample in order to eliminate these two effects. Allison and Pugh[11] described a method for determining the Nernst and Hall coefficients. The transverse electric field is the sum of those due to the Hall and Nernst effects and is given by

$$E_y = (R_o\mu_o H + R_1 M)j_x + (Q_o\mu_o H + Q_1 M)q_x \qquad (3.11)$$

where j_x and q_x are the electric and thermal current densities, respectively. The derivative of the electric field per unit electric current density with respect to B is then

$$\partial(E_y/j_x)/\partial B = (R_o + Q_o q_x/j_x) + \left[(R_1 - R_o) + (Q_1 - Q_o)q_x/j_x\right] \partial M/\partial B. \qquad (3.12)$$

This derivative is usually identified as R_o^* at high fields, so that, if the term containing $\partial M/\partial B$ is negligible, R_o^* is a linear function of q_x/j_x involving only R_o and Q_o. At room temperature Allison mounted the Hall sample vertically and changed the bath and the direction of the electric current in order to vary q_x/j_x for an 80 Ni - 20 Cu sample. The plot of R_o^* versus q_x/j_x was linear, as expected, and yielded values for R_o and Q_o. Similarly, R_1 and Q_1 were obtained from the high field straight line given by Eq. (3.11) with $\mu_o H = B - M$ and $M = M_s$. The errors in the Hall constants due to the Nernst effect were about 5°/o for that sample.

C. Approach to Magnetic Saturation

The law of approach to technical magnetic saturation has been studied extensively, and summaries of theory and experiment have been given by several authors[25,26]. For all materials investigated, the magnetization at high fields is represented quite well by a relation of the general form

$$M = M_s(1 - a/\mu_o H - b/\mu_o^2 H^2) + c\mu_o H.$$

Theoretically, the 1/H term can be attributed to cavities or non-ferromagnetic inclusions, the $1/H^2$ term results from the magnetic crystal forces, and the H term is a "paramagnetic" contribution. Experimental studies have shown that one or two of

---

25/ E. C. Stoner, Rep. Progr. Phys. 13, 83 (1950).

26/ R. M. Bozorth, Ferromagnetism (D. Van Nostrand Company, Inc., New York, 1951).

the constants a, b, and c may be zero depending upon the material and the range of the magnetic field. In many materials, for example, the H term cannot be detected even at high fields, but it is large enough in nickel to be observed quite easily[27]. In iron[28], only the 1/H term was found for $\mu_o H > 0.17$ weber/m^2 ($M > 0.99M_s$), while at lower fields the $1/H^2$ term sufficed (for M up to about $0.98M_s$). Weiss and Forrer[27] had reported the same behavior and had also pointed out that at still lower fields a 1/H dependence again was observed; but the constant a differed from the high field value, and the extrapolation of the straight line plots of M versus $1/\mu_o H$ for the two regions gave different values for M_s.

The approach to saturation in the iron-cobalt alloys was studied by Weiss and Forrer[27]. They found only the 1/H term for $\mu_o H$ between about 0.1 and 1.7 weber/m^2. For the alloys containing between 0 and 95°/o cobalt, a ranged between 0.0004 and 0.002 weber/m^2 and had an average value of about 0.0009 weber/m^2. For the hexagonal alloys (less than 5°/o iron), howev ., a was about 0.02 or 0.025 weber/m^2.

Foner[18] has indicated the possibility of using Hall data to study the high field magnetic properties of materials. Working with exceptionally good Hall data for Armco iron, he evaluated

---

27/ See, for example, P. Weiss and R. Forrer, Ann. Physique 12, 279 (1929).

28/ W. Steinhaus, A. Kuszmann, and E. Schoen, Physik. Z. 38, 777 (1937).

the two Hall constants, using the high field straight line and $M_s = 2.158$ weber/m^2. Then from these constants and the observed values of B and Vt/I he calculated M, $\mu_o H$, and $M/\mu_o H$ and obtained the result shown in Fig. 3.1. The steep straight line near 2.158 weber/m^2 is especially striking. Unfortunately, the study of the approach to saturation in the Hall effect can be extremely treacherous, as will be discussed more fully in Section 6B. The curve of $M/\mu_o H$ versus M obtained by Foner is not real but has the shape expected from the particular treatment given the Hall data. This can be shown quite easily.

The experimentally derived straight line relation between Vt/I and B for high B may be written

$$(Vt/I)_c = C_1 B + C_2. \tag{3.13}$$

The usual assumption is that, in the high field region, $M = M_s$ so that a comparison of Eq. (3.13) with the Hall equation, Eq. (1.2), gives

$$\begin{aligned} C_1 &= R_o^* \\ \text{and} \qquad C_2 &= (R_1^* - R_o^*)M_s. \end{aligned} \tag{3.14}$$

The asterisks denote the experimental values of R_o and R_1 usually published. The magnetization calculated using the Hall equation and the experimental Hall data is

$$M = \left[(Vt/I) - R_o^* B\right] / (R_1^* - R_o^*) \tag{3.15}$$

Substitution from Eq. (3.13) and (3.14) gives the result

$$M = M_s \left[1 + \left\{(Vt/I)_e - (Vt/I_c\right\}/C_2\right] \tag{3.16}$$

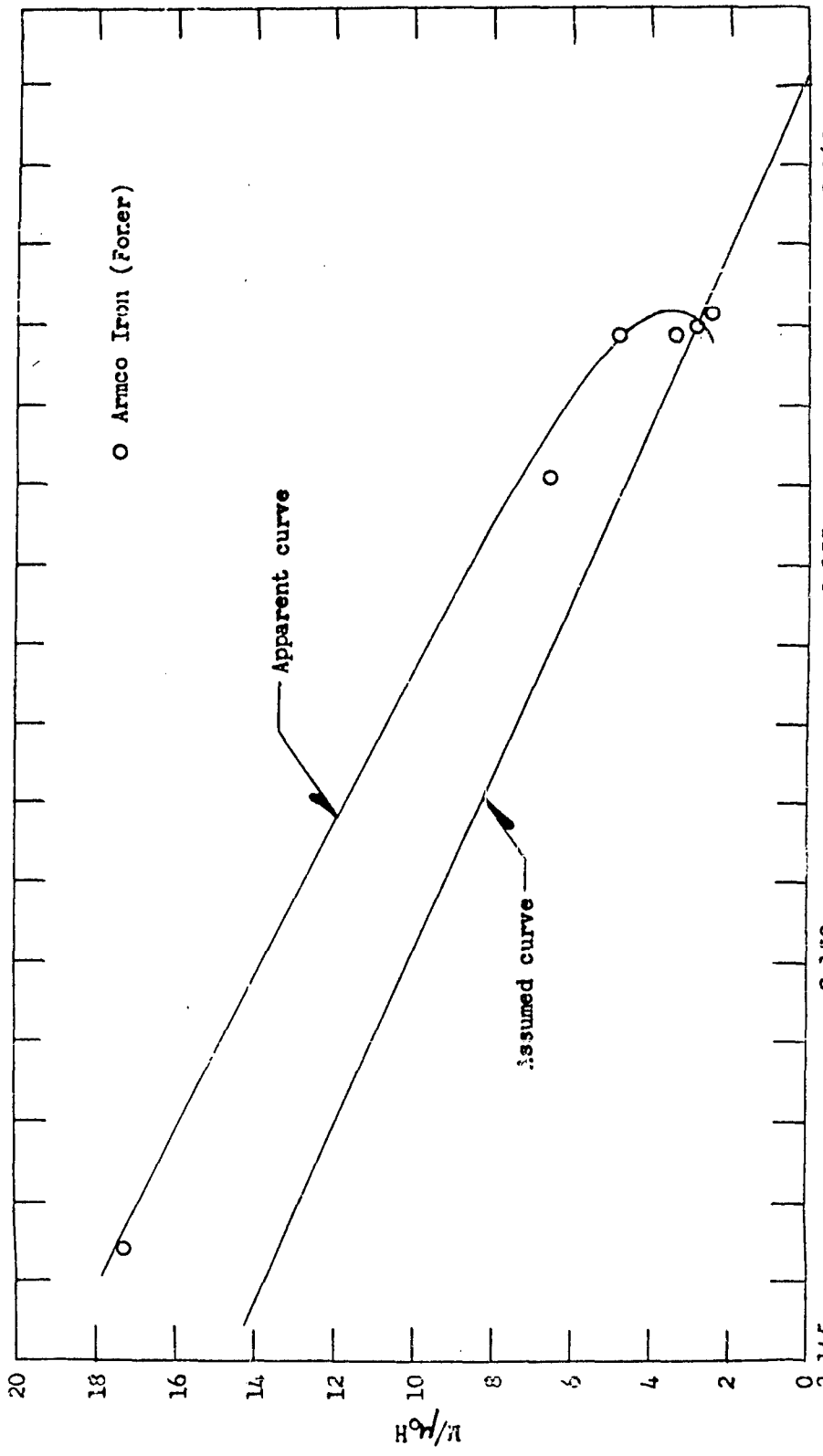

Fig. 3.1 Assumed relation between B and H and the apparent relation calculated from the synthesized Hall data.

where $(Vt/I)_e$ is the experimental value and $(Vt/I)_c$ is the value calculated from Eq. (3.13). Obviously $M = M_s$ for any value of $(Vt/I)_e$ which lies on the high field straight line, and Eq. (3.16) serves only to show the deviations of the experimental Hall data from that line. Since usually the high field data are represented by the "best" straight line, the corresponding values of M would scatter about M_s, giving a vertical line on the $M/\mu_o H$ versus M plot. Foner found such a line and had no reason to suspect it; for, normally, Eq. (3.15) is the most convenient for calculating M from Hall data. Eq. (3.16) was derived almost by accident.

In order to examine more closely what happens when Hall data are treated as described above, a set of data was synthesized. With the assumptions that $R_o = 2.0950$, $R_1 = 63.0414$, and $M = 2.1612(1-0.0011/\mu_o H)$, Vt/I was calculated by Eq. (1.2) for the values of B in Foner's paper. A straight line was then fitted to the four high field points by the method of least squares. From the slope and intercept of this line the "experimental" Hall constants were found to be $R_o^* = 2.4713$ and $R_1^* = 62.9085$. (In finding R_1^*, M_s was taken as 2.1580 and not 2.1612). Finally M, $\mu_o H$, and $M/\mu_o H$ were calculated using Eq. (3.15). The assumed relation between $M/\mu_o H$ and M is shown in Fig. 3.1 along with the apparent relation calculated from the Hall data. The latter curve shows the hook expected near the value of M used as M_s in the calculation of R_1^*.

The approach to magnetic saturation certainly cannot be studied by the method just described. However, since the Hall curves for some of the iron-cobalt alloys do not become straight lines even at the highest fields obtainable, knowledge of the magnetic properties is desirable if not necessary. (For example, note the difference between R_o and R_o^* in the above calculation.) Several methods for studying the Hall effect and the approach to saturation simultaneously are described below; the discussion generally is restricted to the case in which

$$M = M_s(1 - a/\mu_o H)$$

$$= \left[B + M_s - \sqrt{(B - M_s)^2 + 4aM_s}\right]/2 \qquad (3.17)$$

since this law of approach applies to all of the iron-cobalt alloys in the field range of interest.

The validity of Eq. (3.17) would imply its substitution into the Hall relation, Eq. (1.2), and the derivatives thereof:

$$Vt/I = R_o B + (R_1 - R_o)M \qquad (1.2)\ (3.18)$$

$$\partial(Vt/I)/\partial B = R_o + (R_1 - R_o)\partial M/\partial B \qquad (3.19)$$

$$\partial^2(Vt/I)/\partial B^2 = (R_1 - R_o)\partial^2 M/\partial B^2 \qquad (3.20)$$

Experimentally, t and I are known, and V is measured for known values of B. In most cases a plot of Vt/I versus B for high fields is a straight line, which is usually interpreted to mean M is constant ($=M_s$) and the slope is R_o (denoted by R_o^* to allow for the possibility that $\partial M/\partial B$ is constant). R_1 (or R_1^*) is

then obtained from Eq. (3.18) with $M = M_s$. For Armco iron[18] and some iron-cobalt alloys the curvature, Eq. (3.20), is large enough to be observed for the highest fields obtainable, but the presence of the high field straight line in most cases indicates that the experimental errors and sensitivity of the measuring apparatus have made detection of the curvature impossible.

Whenever $a/\mu_o H$ is small Eq. (3.17) can be approximated by

$$M = M_s \left[1 - a/(B - M_s)\right] \tag{3.21}$$

which applies in many cases and is much easier to treat. The substitution of Eq. (3.21) into Eq. (3.18) and the elimination of fractions leads to an equation in observables B and Vt/I which is linear in four "unknowns" involving R_o, R_1, a, and M_s. Obviously the method of least squares can be applied directly to obtain the best values for the four unknowns and, therefore, the desired constants.

A second method, essentially graphical, can be used whenever Eq. (3.21) is applicable and M_s is known. Substitution of Eq. (3.21) into Eqs. (3.18) and (3.19) leads to the results

$$\partial(Vt/I)\partial B = R_o + (R_1 - R_o)aM_s/(B - M_s)^2 \tag{3.22}$$

and

$$(Vt/I) - B\partial(Vt/I)\partial B = (R_1 - R_o)M_s\left[1-a(2B-M_s)/(B-M_s)^2\right] \tag{3.23}$$

The left hand side of Eq. (3.22) is the slope and the left hand side of Eq. (3.23) is the intercept on B = 0 of the line tangent to the Hall curve at the point (B, Vt/I). Obviously, a plot of

the slope of the Hall curve versus $M_s/(B - M_s)^2$ should be a straight line with slope $[(R_1 - R_o)a]$ and intercept R_o, while a plot of the B = 0 intercepts of the tangents to the Hall curve versus $M_s(2B - M_s)/(B - M_s)^2$ should be a straight line with slope $[-(R_1 - R_o)a]$ and intercept $(R_1 - R_o)M_s$.

The method just described gives the unknowns to only three figures when carried out graphically. An alternative procedure is to determine a by this method (which can give M to five figures if M_s and B are known accurately enough) and then obtain R_o and R_1 by fitting the original data.

Whenever the approximation Eq. (3.21) cannot be used, apparently the only method available is the adjusting of the four unknowns M_s, a, R_o, and R_1 to fit the experimental data. The best values for the constants may be obtained by trial and error or by the method of least squares after the Hall equation has been linearized in the standard way.

As an alternative to obtaining the desired constants by fitting Hall data as described above, a better procedure in many cases is simply to correct the experimental values of R_o^* and R_1^*. Writing Eqs. (3.18) and (3.19) for some point in the high field region where the slope of the Hall curve is R_o^* gives

$$Vt/I = R_oB + (R_1 - R_o)M$$

and

$$R_o^* = R_o + (R_1 - R_o)\partial M/\partial B.$$

These equations may be solved simultaneously for R_o and R_1 to give

$$R_o = \left[R_o^* M - (Vt/I)\partial M/\partial B\right] /(M - B\partial M/\partial B)$$
$$\text{and} \quad R_1 = \left[(Vt/I)(1-\partial M/\partial B) - R_o^*(B-M)\right] /(M - B\partial M/\partial B). \tag{3.24}$$

If M is given by Eq. (3.17), Eq. (3.24) becomes

$$R_o = \left[R_o^* M(B + M_s - 2M) - (Vt/I)(M_s - M)\right] /(B-M)(2M-M_s)$$
$$\text{and} \quad R_1 = \left[Vt/I - R_o^* (B + M_s - 2M)\right] /(2M-M_s). \tag{3.25}$$

If Eq. (3.21) is applicable, relatively good approximations of Eq. (3.25) may be written

$$R_o \cong R_o^* - (R_1^* - R_o^*)aM_s/(B - M_s)^2$$
$$\text{and} \quad R_1 \cong R_1^* + (R_1^* - R_o^*)2a/(B - M_s). \tag{3.26}$$

Therefore, if some knowledge of the magnetic behavior is available, the Hall constants may be estimated from the experimental results using Eq. (3.24), (3.25), or (3.26).

4. EQUIPMENT AND EXPERIMENTAL SET-UP

A. The Magnet and Magnetic Fields

The magnetic fields were obtained with the Arthur D. Little Company magnet[29] and the auxiliary equipment described in detail by S. Foner[30]. Some modifications of the system were necessary and are described below.

P. Cohen[8] pointed out that intermittent shorts from the magnet coils to ground had led to unstable operation of the control circuits and had necessitated several changes in the negative feedback loop. Fluctuations in magnet current were not completely eliminated, however, and the situation became progressively worse as the resistance from coils to ground continued to decrease. Finally, for one coil in each yoke, the resistance to ground was less than ten ohms and operation was discontinued.

The yokes were disassembled and the low resistance shorts were immediately found; arcing from the coils to the yokes had resulted in the breakdown of the micarta insulation. Several parts of the system were corroded, and fine particles of rust and a small amount of water containing acid were found in the silicone oil coolant.

No leaks were found in the heat exchanger, the most likely source of water, and the presence of water was finally attributed

---

29/ F. Bitter and F. E. Reed, Rev. Sci. Inst. 22, 171 (1951).

30/ Simon Foner Thesis, Navy Contract Nonr-206(00) Technical Report No. 2, June 1952.

to condensation of water vapor trapped in the system. The rust in the oil apparently had come from the few unplated steel parts in the system, and the contamination had caused arcing.

The yokes were cleaned and reassembled after the remaining steel parts in the system had been cadmium plated. To prevent a recurrence of the trouble, a silica gel basket was installed in the reservoir at the intake of the oil pump to absorb any water which might get into the oil, and a filter was installed to remove particles of matter from the oil[31]. Before the yokes were reconnected the oil lines to the magnet were joined, and the system was flushed. After the magnet was put back into operation the resistance from the coils to ground was better than a megohm, and the stability of the control circuits was quite satisfactory.

Some fluctuations in magnet current were still observed, however, and F. Ryan traced them to two sources. First, the commutator of the dc generator was worn, and fluctuations were introduced by the faulty contact of the brushes. This condition was eliminated through machining of the commutator, a standard maintenance practice. The second source lay in the natural loop in the control system. Any fluctuation within the system, such as one due to insufficient regulation of the power supply, was amplified and appeared everywhere in the loop, which

---

31/ The filter is a Purolator Micronic Filter with a capacity of 150 gal/min. In company tests with a fine dust of known size distribution, the filter element removed 99% of particles between 5 and 10 microns and 99.8% of particles 10 microns and larger.

had a relatively fast response. This difficulty was eliminated quite easily; the negative feedback was no longer needed, so the grid of the final amplifier stage was disconnected from the magnet coils and connected instead to the common of the amplifier (-110 v dc, with the chassis at ground) through a potentiometer and a 0.5μf condenser. The system is now much slower, but is very stable.

Due to the high saturation magnetization of the iron-cobalt alloys and the (magnetically) unfavorable sample geometry, the magnetic fields required were the maximum obtainable with the A. D. L. magnet. The 5-3/4 in. face diameter, tapered pole pieces were used with the smallest gap practical - 5/8 in. Before the magnet was repaired the controller would not function in the highest field position (110 kw operation) and only 3.1 weber/m^2 (35 kw operation) could be obtained; afterward, however, the operation at the highest position was quite stable so that fields up to 3.3 weber/m^2 could be used.

The fields were measured with two different Rawson rotating coil fluxmeters calibrated with a 1000 gauss standard magnet, also obtained from the Rawson Electrical Instrument Company. The field is uniform to well within 1°/o over a region 4 in. in diameter, which is 1-1/2 in. larger than the sample diagonal. Field measurements agree to 1°/o or less, and subsequent observations have indicated that much of this variation may be due to the fluxmeters and not the field control. The magnet

repair and circuit modification resulted in changes of a few per cent in the low fields but had no detectable effect on the high fields.

With the fluxmeters used, no hysteresis can be observed in the magnet; but, for consistency, the cycling procedure used during field measurements was the same as that used for the Hall measurements.

B. The Dewar

Hall measurements at low temperatures were desired, but a maximum field of only 2.6 weber/m^2 could be obtained with the 2 in. gap required by the existing low temperature apparatus. Furthermore, thermal isolation of some samples was necessary even at room temperature. Hence, a special dewar was built to fit into the 5/8 in. gap needed. It was quite satisfactory when holding liquid nitrogen (77°K) or liquid ethyline[32] (169°K) as well as when used at room temperature with a silicone oil which has a low viscosity and a high thermal conductivity[33]. Liquid nitrogen boiled off at less than one liter per hour during measurements of the Hall effect.

The specially constructed dewar is double-walled with the space between the walls evacuated. It is made from two similar

---

32/ Ethylene was liquified by passing it through a cold trap immersed in liquid nitrogen.

33/ Several other baths were tried--dry ice and acetone, dry ice and methanol, dry ice and silicone oil, liquid-solid methanol, and liquid-solid silicone oil--but temperature variations were so large that the measurement of the Hall potential was impossible.

brass containers, one fitting inside the other with no contact between them except where they are joined at the top. The lower part of each container is rectangular in cross-section while the upper part is cylindrical. Thus, the lower part of the dewar fits into the 5/8 in. magnet gap, and the upper part provides a reservoir of about two liter capacity.

In order to reduce the heat conduction down the inside wall of the dewar, a 7 in. length of the wall was machined to a thickness of 0.020 in.

The working space provided by the inner "box" (i.e. the lower section of the inside container) is about 4 in. high and 2-7/8 in. x 3/8 in. in cross-section. Overall, the outer box is about 8 in. high, 4 in. wide, and 5/8 in. thick.

The flat sides of each box are necessarily thin (0.033 in. and 0.041 in. thick for the inner and outer boxes, respectively), and are subject to forces of several hundred pounds when the space between the walls is evacuated. To offset the effects of atmospheric pressure, there are spacers between the flat walls of the two boxes. The spacers are micarta rings 0.052 in. high; they are flat on one end and have fillets on the other to reduce the area of contact and, consequently, the heat leak. The spacers do prevent contact between the walls; but the walls are somewhat deformed, and in some places the walls of the inner box are squeezed inward, reducing the 3/8 in. working space almost 1/32 in.

Initially the cross-section of each box was as shown in Fig. 4.1a. A U-shaped frame was fabricated using a silver solder, walls of sheet brass were soft soldered to the frame, and the assembly was soft soldered into the cylindrical top section. The low melting point solder was used to minimize distortion. The dewar worked quite well for about a year; then the seams of the boxes failed. The cause is not known but perhaps there were phase transformations in the solder, or there may have been mechanical failure resulting from the pressure on the walls or from repeated shocks caused by thermal changes.

The bottom sections were rebuilt, and two designs were used. As indicated in Fig. 4.1b the inside box was made from two pieces, each milled from thick sheet brass. The two halves were clamped together and silver soldered, and the assembly was silver soldered into the cylindrical top section. The outside box was made from three pieces, as shown in Fig. 4.1c. A U-shaped frame was fabricated with a silver solder melting at 1270°F, and the walls were cut from 0.041 in. sheet brass. The walls and the frame were clamped between two sheets of transite and were soldered with a silver solder melting at 1145°F. The assembly was then fastened into the top section with the low-melting-point silver solder.

The latter method was better for two reasons. First, contrary to expectations, it yielded a box which was almost free from distortion; while the thin walls of the inner box, made by

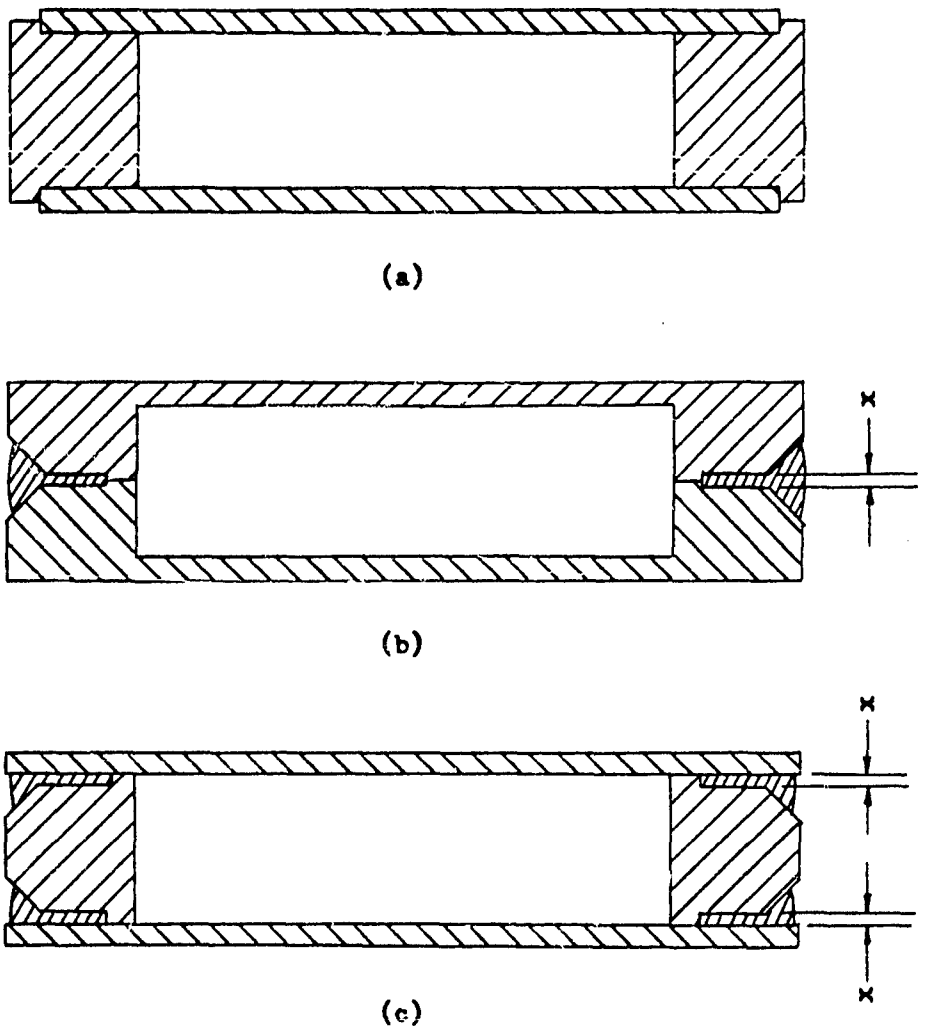

Note: Dimension x is 0.005 - 0.010 inch to provide for strong soldered joints.

Fig. 4.1 Cross-sections used in the construction of the box-like bottom sections of the dewar.

the other method, had irregularities caused by machining and made worse by soldering. Second, the occurrence of a leak is less likely in the thin walls of the box made by the latter method since the thin sheet is less porous than the thick sheet brass.

C. Sample Mounting

The sample holder, consisting primarily of two rigidly mounted sample current electrodes and two micarta guides, provided quite simply for alignment of the sample in the magnet; the guides fitted snugly inside the dewar, and the dewar fitted snugly between the pole pieces.

Two different experimental set-ups were used, both providing for elimination of the Ettingshausen and Righi-Leduc effects.

For the unannealed samples the technique was that used by Cohen[8] and Allison[11]. A sample (basically a flat plate 2 cm wide, 6 cm long, and 1 mm thick), four probes, and wires were made from each alloy. The sample was fastened to the sample current electrodes with pressure contacts. The probes were square and were beveled at one end to provide a line contact on the edge of the sample. They were positioned by slots in a micarta framework fastened to the sample current electrodes, and were pressed against the sample with L-shaped micarta clamps instead of the usual phosphor-bronze springs. A small machine screw held each clamp and probe tightly in place, the one leg of the clamp serving as a fulcrum. A piece of alloy wire was

soldered to each probe[34/], and the junctions[34/] of the alloy wires and the copper leads were placed inside a copper box to eliminate thermal emf's. Two of the probes, opposite each other on the center line of the sample, were used to measure the Hall potential; and the two others, located 2 cm apart on one side of the sample, were used for resistivity measurements. A thermocouple was located at each end of the sample in a slot between it and the copper bar clamping it to the sample current electrode.

The technique used with the annealed samples eliminated the need for probes. Samples the same size as above were made, but then the edges were machined to leave four lugs which replaced the probes. Each lug was about 0.035 in. wide and protruded about 1/16 in. from the sample. A piece of the alloy wire was spot-welded to each lug, and the junctions[34/] with the copper leads again were placed in a copper box to eliminate thermal emf's. The thermocouples were clamped independently to the sample, and a major part of the sample was clamped between two brass sheets (insulated from the sample with mica) to improve rigidity and reduce thermal gradients in the bath.

Each system has certain advantages and disadvantages. The former provides for definite lines of contact between sample and probes, but requires a framework to support the probes. The latter system permits better mounting of the thermocouples and

---

34/ A solder having a low thermal emf against copper was used for consistency.

is more adaptable to high temperature work but does not define as accurately the points of contact for the potential leads. Also, the assembly of sample and wires is very difficult to mount when the sample material is brittle.

D. Samples

Nine iron-cobalt alloys (0.1, 0.5, 15, 35, 60, 70, 75, 80, and 85°/o cobalt) were furnished in ingot form by Westinghouse Electric Corporation. Material for a cobalt sample was cut from an ingot of cobalt furnished by the Allegheny Ludlum Steel Corporation.

With a little care, probes and samples of both types were machined from even the most brittle of the alloys. Wires were made easily by cold-drawing for all but the 35 and 60°/o cobalt alloys and the cobalt. Using the results of Ellis[35] as noted by Bozorth[36], a piece of the 60°/o alloy was hammered while hot and then water quenched and wires were cold-drawn from this material. Both the 35°/o alloy and the cobalt were extremely brittle and could not be cold-drawn; a thin sheet of each was hot-rolled, and narrow strips cut from them were used as wires.

The six unannealed samples on which measurements were made (0.1, 60, 70, 75, 80, and 85°/o cobalt) were machined from the

---

35/ W. C. Ellis, Rensselaer Polytech. Inst. Bull., Eng. Sci. Ser. 16, 1 (1927).

36/ Reference 26, p. 192.

original ingots. The histories of the annealed samples differed and are given below:

0.1°/o Cobalt. The unannealed sample was modified and annealed.

0.5°/o Cobalt. The same as for the 0.1°/o sample.

15°/o Cobalt. A full-size sample could not be cut from the original ingot, so a small quantity of the material was remelted in a vacuum induction furnace. The sample was cold-rolled to rough size from part of the new ingot, machined, and annealed.

35°/o Cobalt. The same as for the 0.1°/o sample.

60°/o Cobalt. Due to its brittleness the unannealed sample split while being modified. Another full-size sample could not be obtained from the ingot, so a small amount of material, including the original sample, was remelted in the vacuum induction furnace. A sample was hot-rolled to rough size, machined, and annealed.

70°/o Cobalt. The same as for the 0.1°/o sample.

75°/o Cobalt. The same as for the 0.1°/o sample.

80°/o Cobalt. The unannealed sample was destroyed when an annealing furnace burned out. A new sample was cut from the original ingot and annealed.

85°/o Cobalt. The same as for the 80°/o sample.

Cobalt. The only full-size sample which could be cut from the original piece of material was destroyed in the annealing furnace. The remaining material was remelted in the vacuum induction furnace, hot-rolled to rough sample size, machined, and annealed.

The samples were homogenized and annealed in dry hydrogen for a week at 1200°C and furnace cooled at less than 1°C per minute. They were reheated and held at 700°C for two hours in vacuum in order to remove any hydrogen, and again the furnace was cooled at less than 1°C per minute. In their work on the iron-cobalt phase diagram, Ellis and Greiner[37] found that the alloys showing order-disorder behavior were well ordered when cooled at less than 3°C per minute. Thus, the cooling rate used here should have produced well ordered samples. The vacuum treatment was based on Newell's[38] work on hydrogen absorption and should have removed all hydrogen.

E. Physical Measurements on Samples

Sample lengths and widths were measured with micrometers and were known to about 0.1°/o and 0.3°/o respectively. Sample thicknesses were measured using a Pratt and Whitney Electrolimit Gauge designed to indicate deviations (0.002 in. full scale) from a pre-set dimension (in this case a thickness set with gauge blocks); they were known to about 1°/o.

Sample densities, calculated from the masses and the measured sample dimensions, are known to about 1°/o. They are listed in Table 4.1 with the results of Weiss and Forrer[27].

37/ W. C. Ellis and E. S. Greiner, Trans. Am. Soc. Metals 29, 415 (1941).

38/ W. C. Newell, J. Iron and Steel Inst. 141, 243 (1940).

Table 4.1 Sample Density and Saturation Moment per Gram for the Iron-Cobalt Alloys

	Density (gm/cc)			Saturation Moment per Gram* (erg/gauss-gm)			
% Co	As Cast	Annealed	Ideal*	77°K	169°K	283°K	303°K
0.1	7.82	7.79	7.86	221.5	220.4	217.9	217.4
0.5	7.81	7.79	7.86	221.9	220.8	218.3	217.8
15	7.84	7.86	7.93	236.0	235.1	232.8	232.3
35	8.00	7.97	8.07	241.1	240.5	239.0	238.7
60	8.18	8.22	8.32	223.6	223.0	221.9	221.6
70	8.32	8.28	8.45	211.4	210.9	209.6	209.3
75	8.39	8.34	8.51	205.0	204.5	203.2	202.9
80	8.42	8.47	8.57	188.6	187.9	186.3	185.9
85	8.53	8.55	8.65	181.9	181.2	179.5	179.1
100	8.76	8.82	8.87	163.3[a]	162.2[a]	159.6[a]	159.1[a]

* Reference 27.

a Reference 26, p. 194 and p. 279.

The spacing between contacts used for resistivity measurements was determined with a traveling microscope. The marks made on the samples by the probes ranged in width from 0.002 cm to 0.012 cm and had an average width of 0.006 cm, representing an error of about 0.3°/o in the spacing. Thus, the absolute resistivities of the unannealed samples are known to about 1°/o. On the basis of the 0.035 in. wide lugs used, however, the error in the absolute resistivities of the annealed samples could be as large as 5°/o, but the relative resistivities are probably known to far greater accuracies.

F. Saturation Magnetization

The values used for the saturation magnetization of the nine iron-cobalt alloys were based upon the results of Weiss and Forrer[27] who measured the magnetization of iron, cobalt, and twenty-five alloys as a function of both H and T. If $\sigma_{H,T}$ is the magnetic moment per gram[39] at field H and absolute temperature T, they found that

$$\sigma_{H,T} = \sigma_{\infty,T}(1 - a/H)$$

and

$$\sigma_{\infty,T} = \sigma_{\infty,0}(1 - AT^2) \qquad (4.1)$$

for fields between 1000 and 17000 oersteds and temperatures between 77 and 300°K. A was calculated from values of $\sigma_{\infty,0}$ and $\sigma_{\infty,288}$ obtained from plots of their data; and $\sigma_{\infty,T}$ was calculated

---

39/ In this section quantities are expressed in Guassian units.

using Eq. (4.1). $4\pi M_S$ for the nine alloys was then calculated from $\sigma_{\infty,T}$ using the relation $(4\pi M_S)_T = 4\pi \sigma_{\infty,T} d_T$, where d_T is the density at temperature T.

The values of $\sigma_{\infty,0}$ and $\sigma_{\infty,288}$ for the cobalt sample were taken from Bozorth[40], and the calculation was completed in the same way.

The values of $\sigma_{\infty,T}$ used for 77, 169, 283, and 303°K are listed in Table 4.1. The number of Bohr magnetons per atom in terms of σ is $A\sigma/N_0\beta$, where A is the atomic mass, N_0 is Avagadro's number and β is the Bohr magneton ($=9.273 \times 10^{-21}$ erg/gauss).

G. Measuring Circuit

A block diagram of the measuring circuit is shown in Fig. 4.2. Six double-pole-double-throw switches were arranged to permit the use of either of two potentiometer circuits for standardizing the field control (98.90 mv between two fixed points in a voltage divider network) and for measuring the sample current (IR drop across a 50 mv, 30 amp shunt), sample resistance (IR drop between two probes), the temperature (thermocouple emf) at each end of the sample, and the Hall potential. Two probes were used for Hall potential measurements, and the reversal in sign of the Hall potential with magnetic field was offset with a bias voltage introduced into one Hall-potential lead. The bias circuit can give a maximum of about 60 μv bias with either polarity.

40/ Reference 26, p. 194 and p. 279.

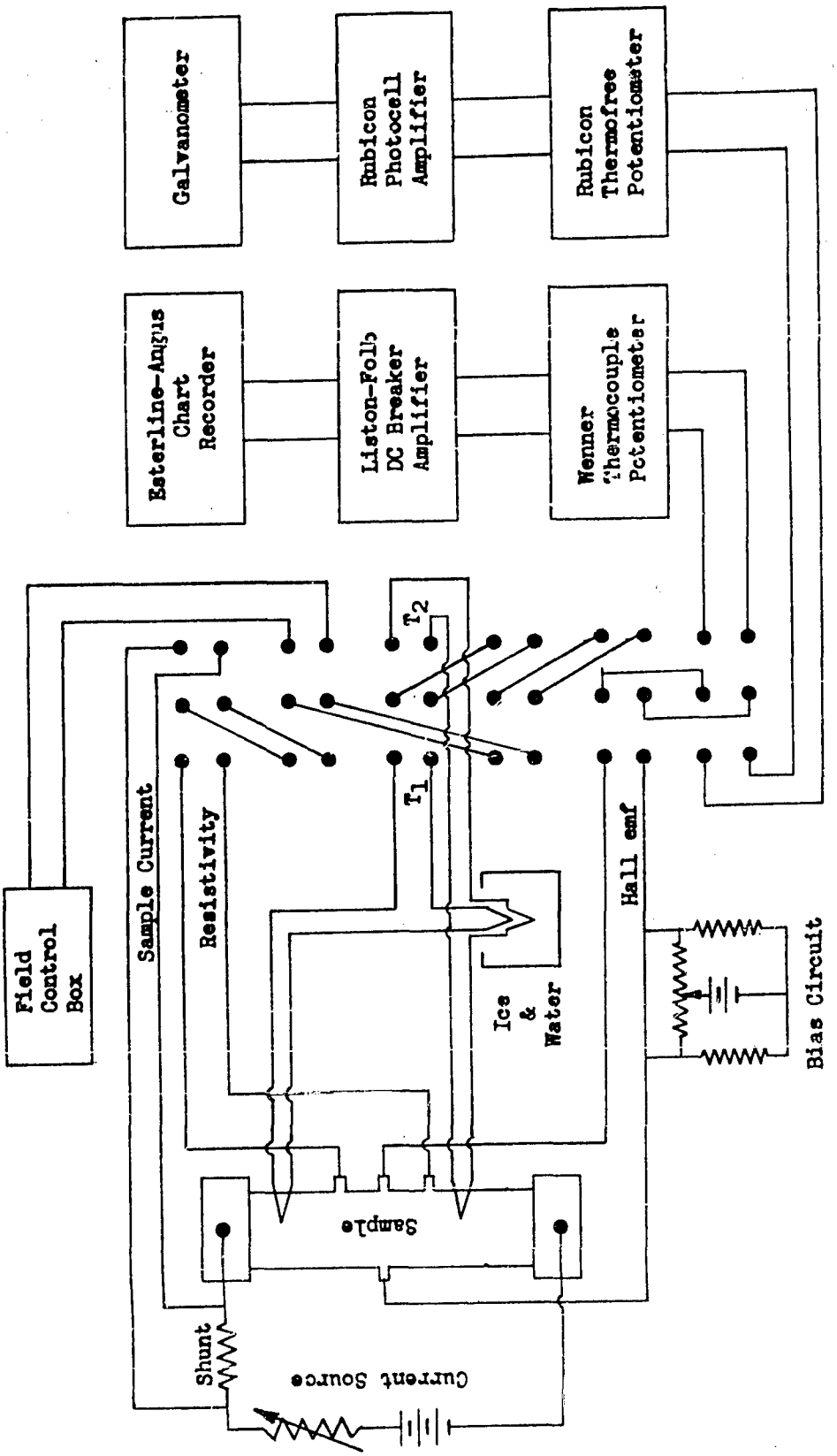

Fig. 4.2 Schematic measuring circuit.

The circuit based on the Leeds and Northrup Wenner Thermocouple Potentiometer has been described in detail by Foner[9,30]. With reduced amplifier gain this circuit serves quite well as a null system for measuring everything but the Hall potential[41]; with high gain, the smallest change possible on the potentiometer (10^{-7}v) appears as a step (usually chosen to be about 1 in.) on the chart.

In contrast to the Wenner Potentiometer, the Rubicon Thermofree Potentiometer has 1/10 the range and provides for continuous potential settings; the amplifier and galvanometer are used to indicate the null setting. The Rubicon "Photoelectric Galvanometer and Amplifier Assembly" consists of a light source, a reflecting galvanometer, twin photocell circuits, and a single-stage, differential amplifier. The input is connected to the galvanometer so that a change in input potential changes the relative illumination of the two photocells. Normally the resulting unbalance in the photocell circuits is then amplified and fed to an external output galvanometer; but, for Hall measurements, the above arrangement was modified to eliminate the amplifier. The photocells and their load resistors were used simply as a high

---

41/ When the field control was standardized, it had to be disconnected from the rest of the magnet control circuit to prevent the introduction of a second ground into the amplifier circuit.

resistance bridge, and a reflecting galvanometer with high current sensitivity (in series with a high resistance) was used to indicate the unbalance of the bridge.

The two potentiometer circuits had about the same sensitivity (2×10^{-9} volt), and either could be used to measure Hall potentials. However, the latter has proved to be better. It is much faster; for potentials can be read directly, and the need for interpolation from the recorder charts is eliminated. Also, it has a slower response, so that more of the noise is eliminated and the null can be obtained quickly. In some cases the charts obtained with the Wenner circuit showed a noise level of almost 10^{-7} volt, necessitating a long recording period for each potential measurement and requiring interpretation of the trace. Finally, the use of the null system eliminates any non-linearity in the amplifier or galvanometer.

H. Measuring Procedure

The transverse potential was measured by the incremental method used by other investigators[42]. The field cycling sequence used is R7-L7-R7-L7-R7-L7-L9-L7-L8-L7-L6-etc. through L1 and L1/2, a second set of R7-L7 reversals, a corresponding R sequence, and a third set of R7-L7 reversals[43]. A reference

---

42/ See, for example, reference 18.

43/ In the notation Rx and Lx, R and L denote the two field directions, and x denotes the switch position set on the field control box.

point is obtained from the field reversals, and the addition of the potential increments to the reference potential gives the transverse potential as a function of magnetic induction.

The cycling procedure above provides for the elimination of drift in the reference potentials, and the averaging of the results for the two field directions eliminates potentials which are even functions of the magnetic field. The use of increments rather than reversals at each field position eliminates the error in R_o^* due to the temperature dependence of R_1. (In some cases, if only reversals were used, a systematic change in temperature of 1°C could lead to an error of as much as $2 \times 10^{-11} m^3/coul$ in R_o^*.)

The sample current and temperatures were measured whenever field reversals were made, so that the average temperature and average reference potential for a run would correspond.

5. EXPERIMENTAL RESULTS

Using the method described in Section 4H the Hall potential was measured at 77°K, 169°K, and room temperature for values of magnetic induction, B, between 1.2 and 3.3 weber/m^2. The results are shown in Figs. 5.1 to 5.13, where V is the Hall potential, t is the sample thickness, and I is the sample current. In most cases the high field region of the curves can be represented quite well by straight lines; but Figs. 5.2, 5.4, and 5.6 reveal that, as expected, saturation was not reached in the 0.1, 0.5, and 15°/o cobalt alloys. Also, as expected, the initial slope of the curves for a given material is strongly dependent on temperature while the high field slope is relatively temperature independent.

The resistivity as a function of temperature and composition is shown in Fig. 5.14. For the mid-range of composition the curves show the well known minimum due to the ordering which occurs in these alloys.

The ordinary Hall coefficient, R_o^*, was calculated using Eqs. (3.13) and (3.14) and is shown[44] in Fig. 5.15 with the results given by Foner and Pugh[9], Foner[45], and

---

44/ 10^{-13} v-cm/amp-gauss = 10^{-11} m^3/coul.

45/ S. Foner, Phys. Rev. 99, 1079 (1955).

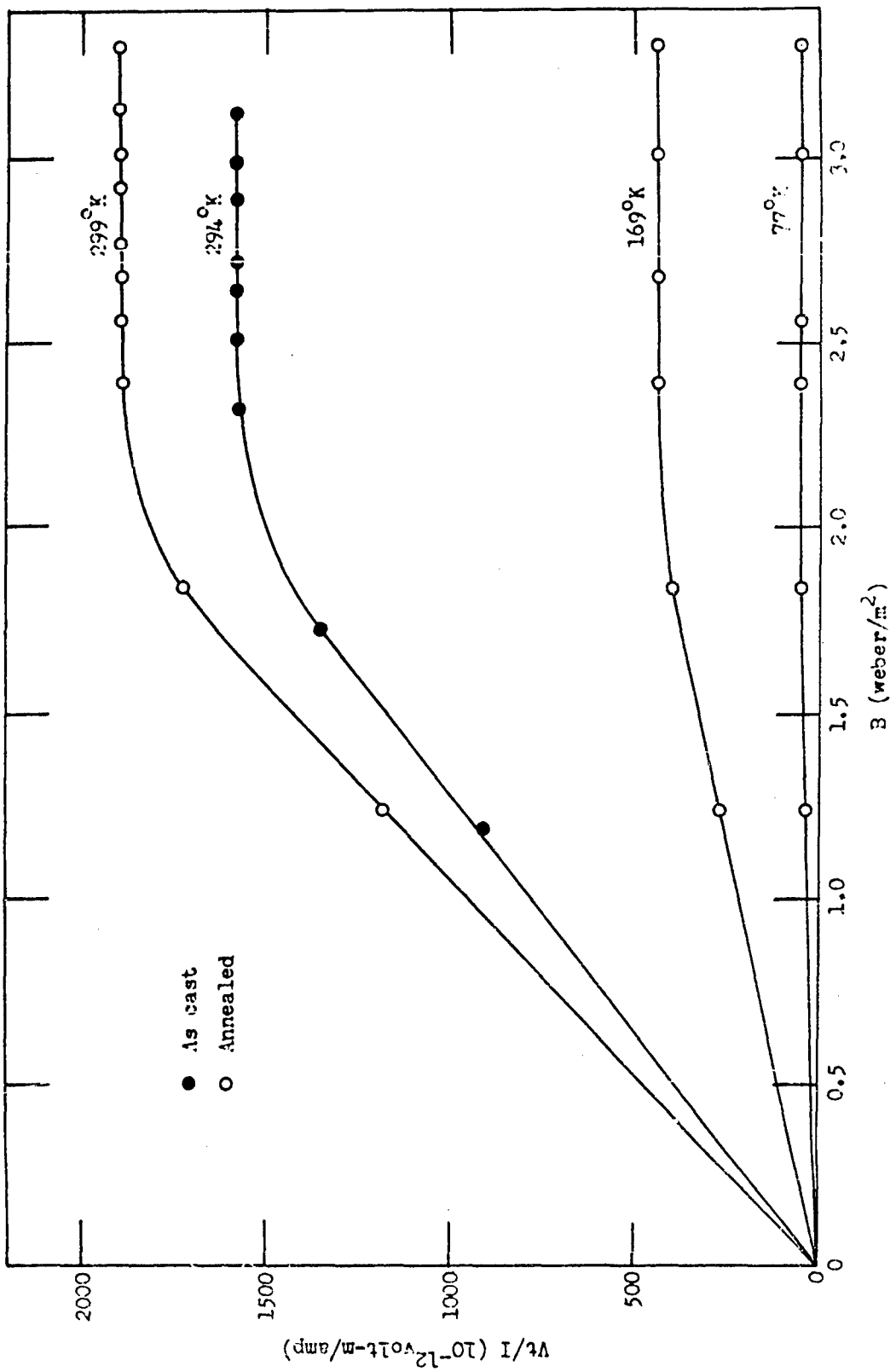

Fig. 5.1 Hall electric field per unit current density as a function of magnetic induction for 0.1% Cobalt - 99.9% Iron.

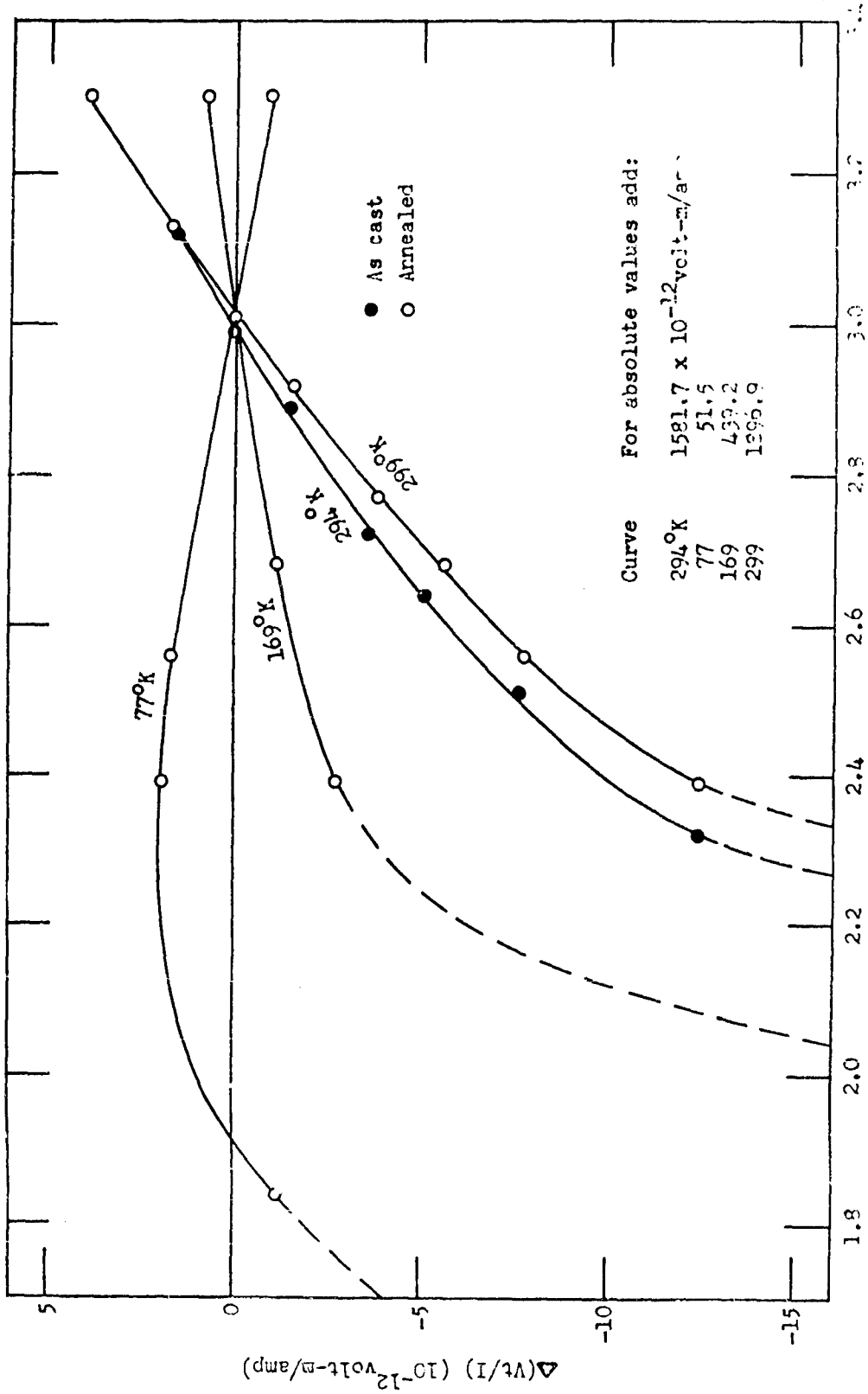

Fig. 5.2 High field region for 0.1% Cobalt - 99.9% Iron expanded to show details.

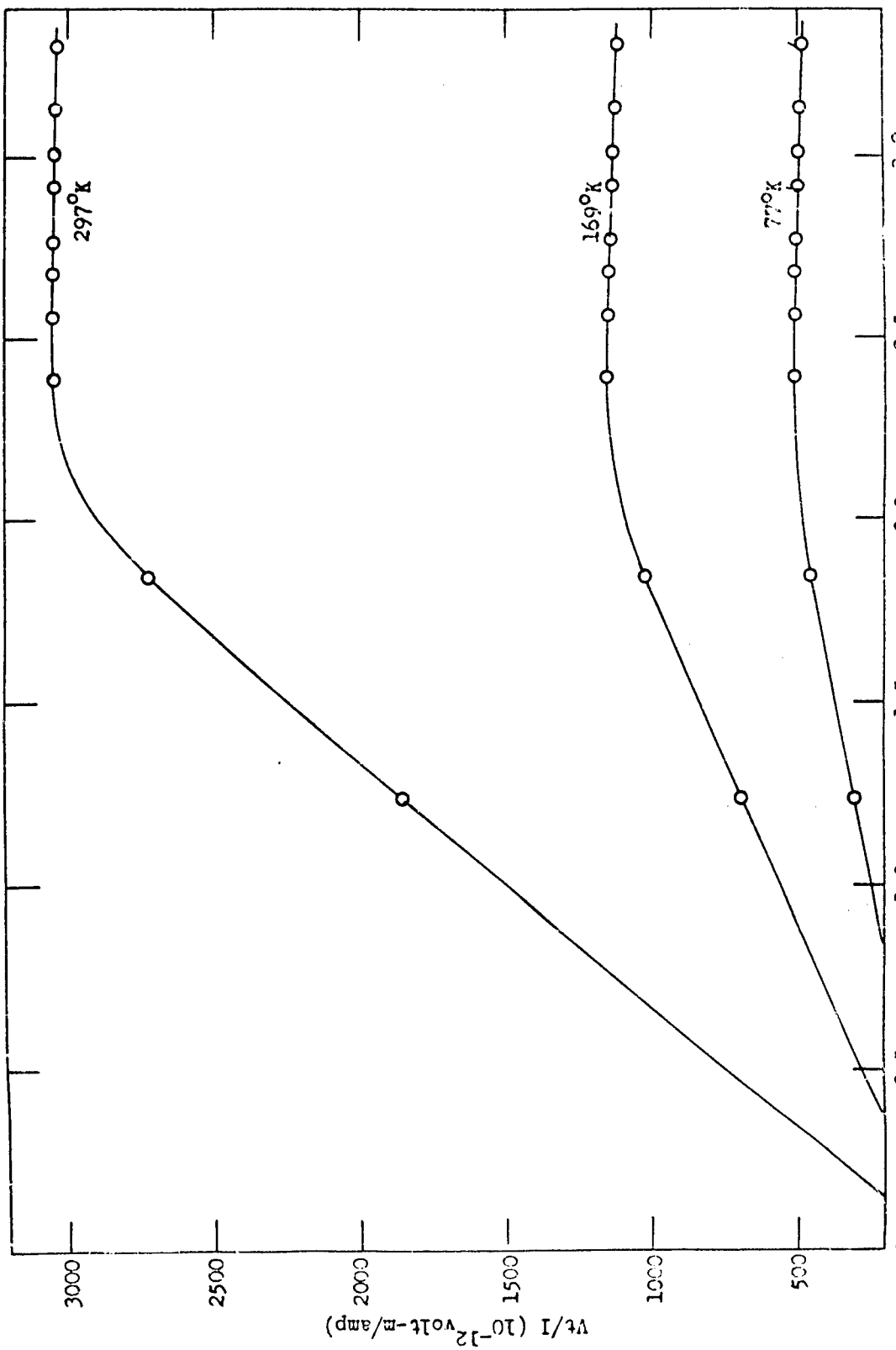

Fig. 5.3 Hall electric field per unit current density as a function of magnetic induction for 0.5% Cobalt - 99.5% Iron (annealed only).

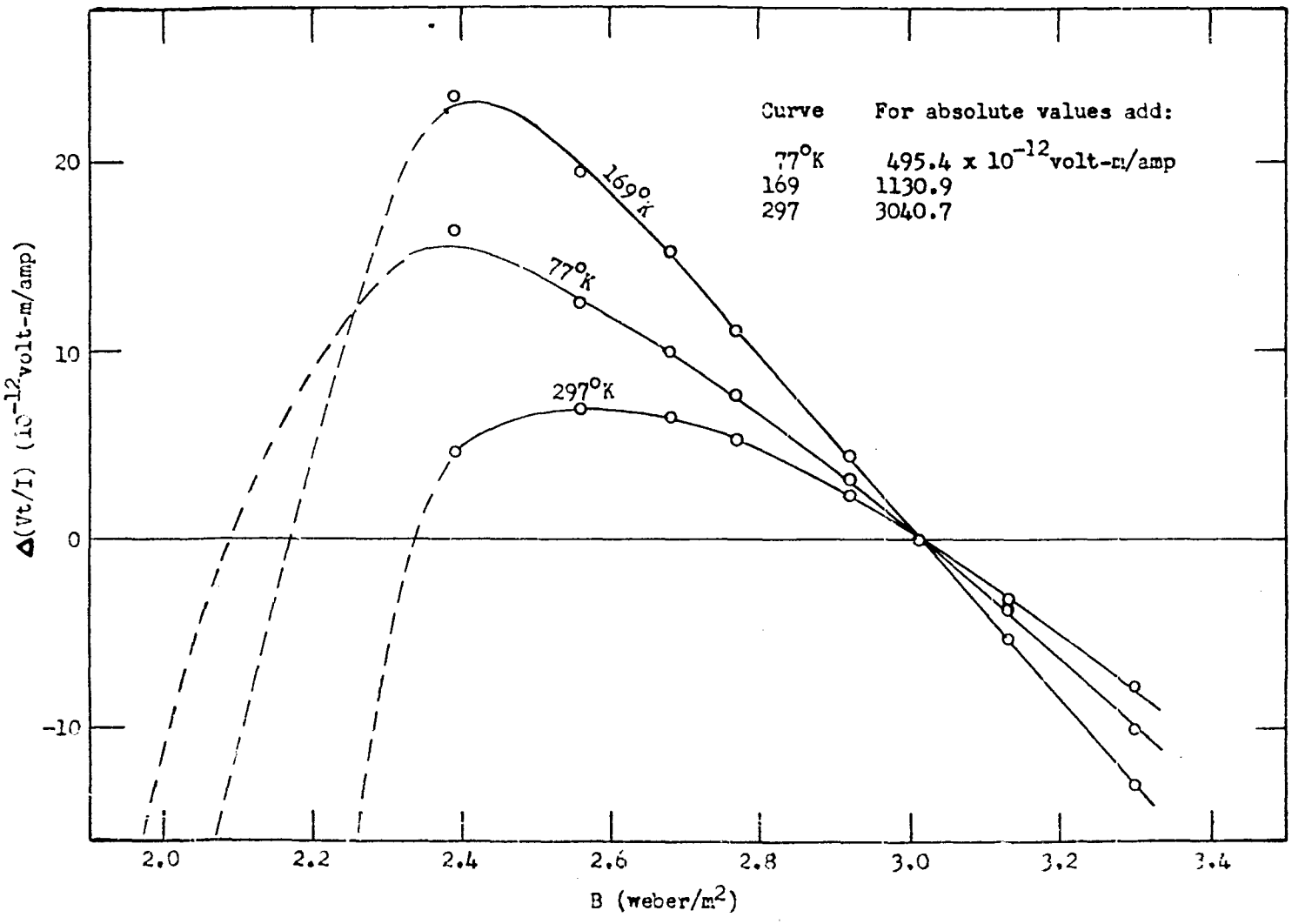

Fig. 5.4 High field region for 0.5% Cobalt - 99.5% Iron expanded to show details.

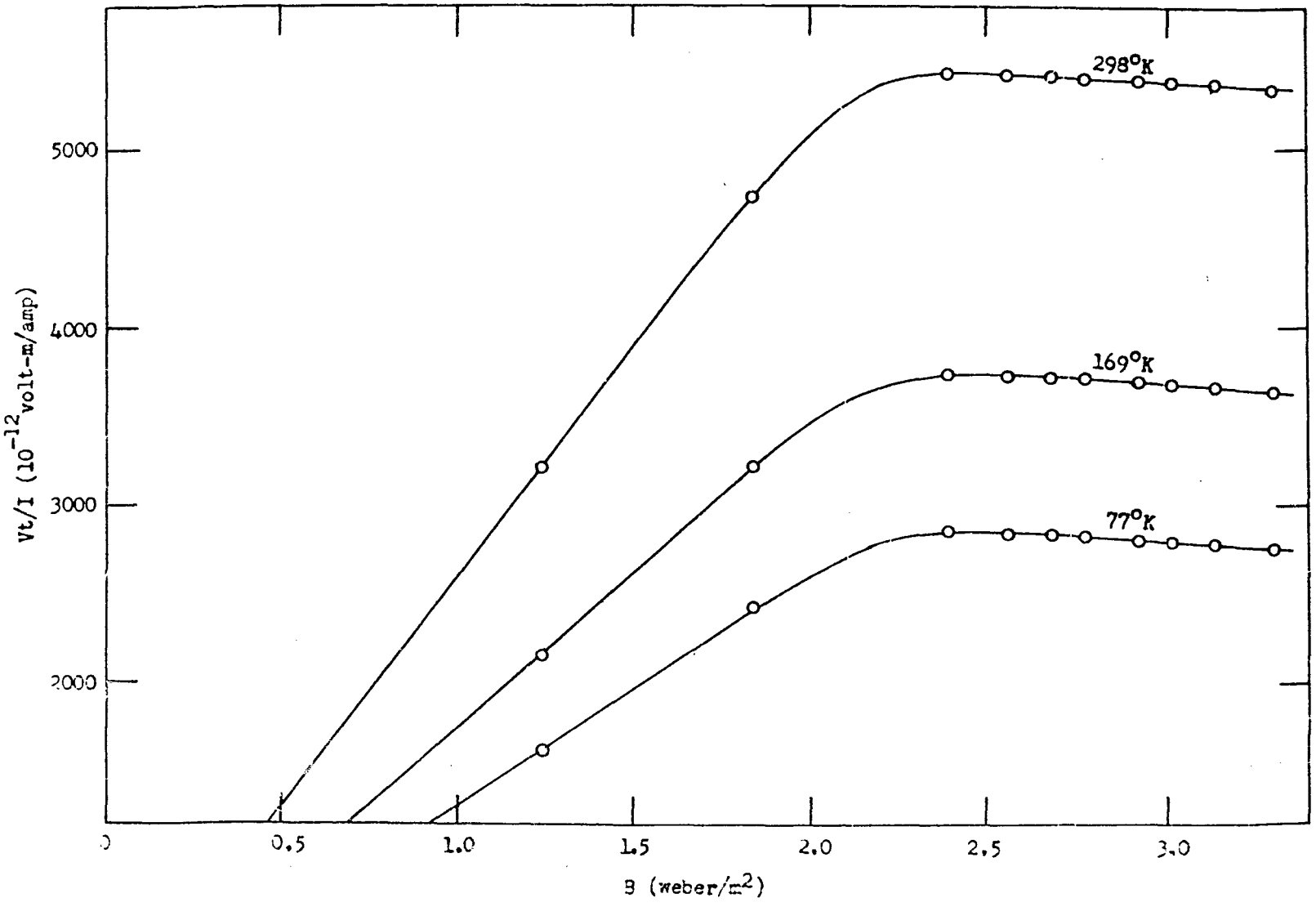

Fig. 5.5 Hall electric field per unit current density as a function of magnetic induction for 15% Cobalt - 85% Iron (annealed only).

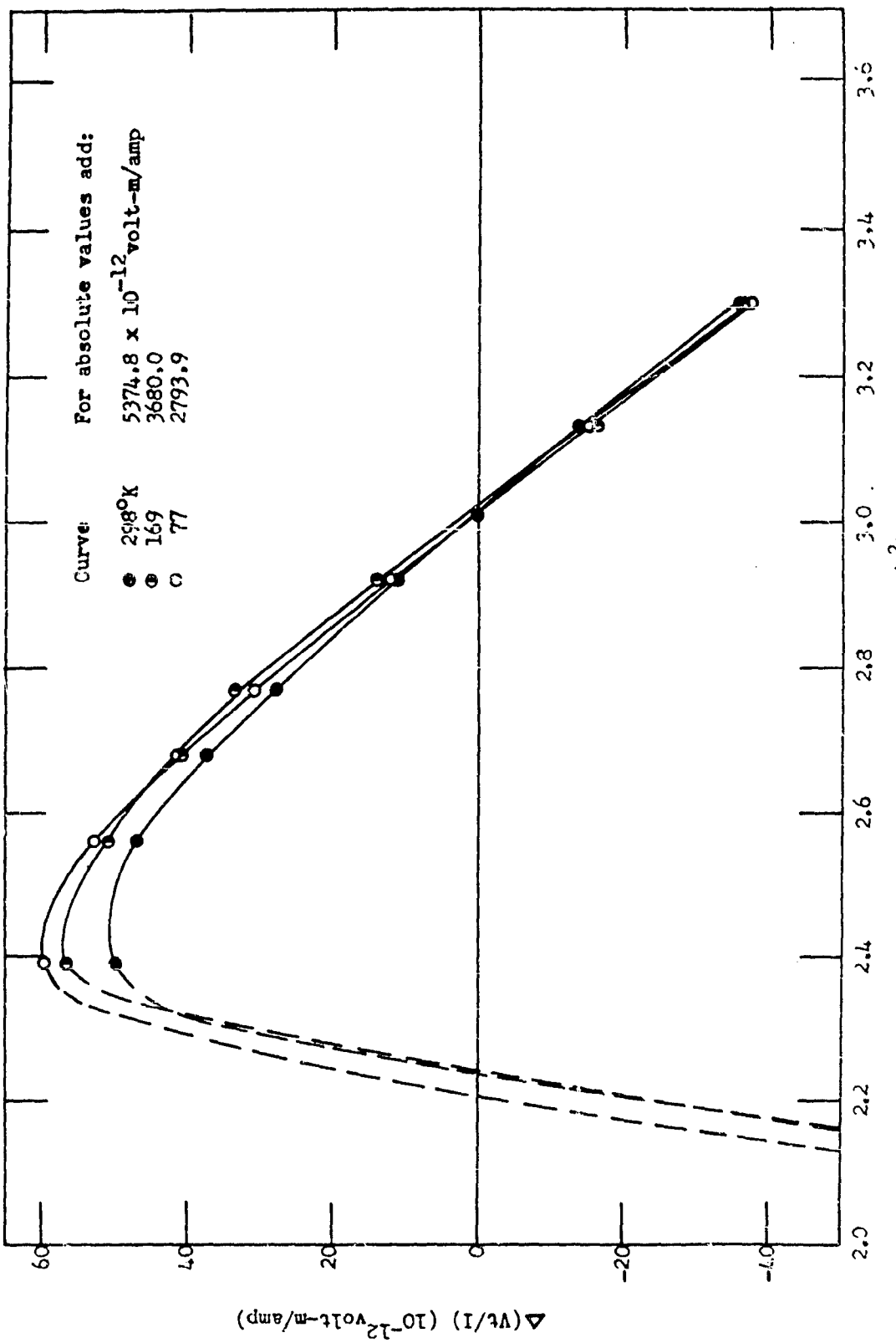

Fig. 5.6 High field region for 15% Cobalt - 85% Iron expanded to show details.

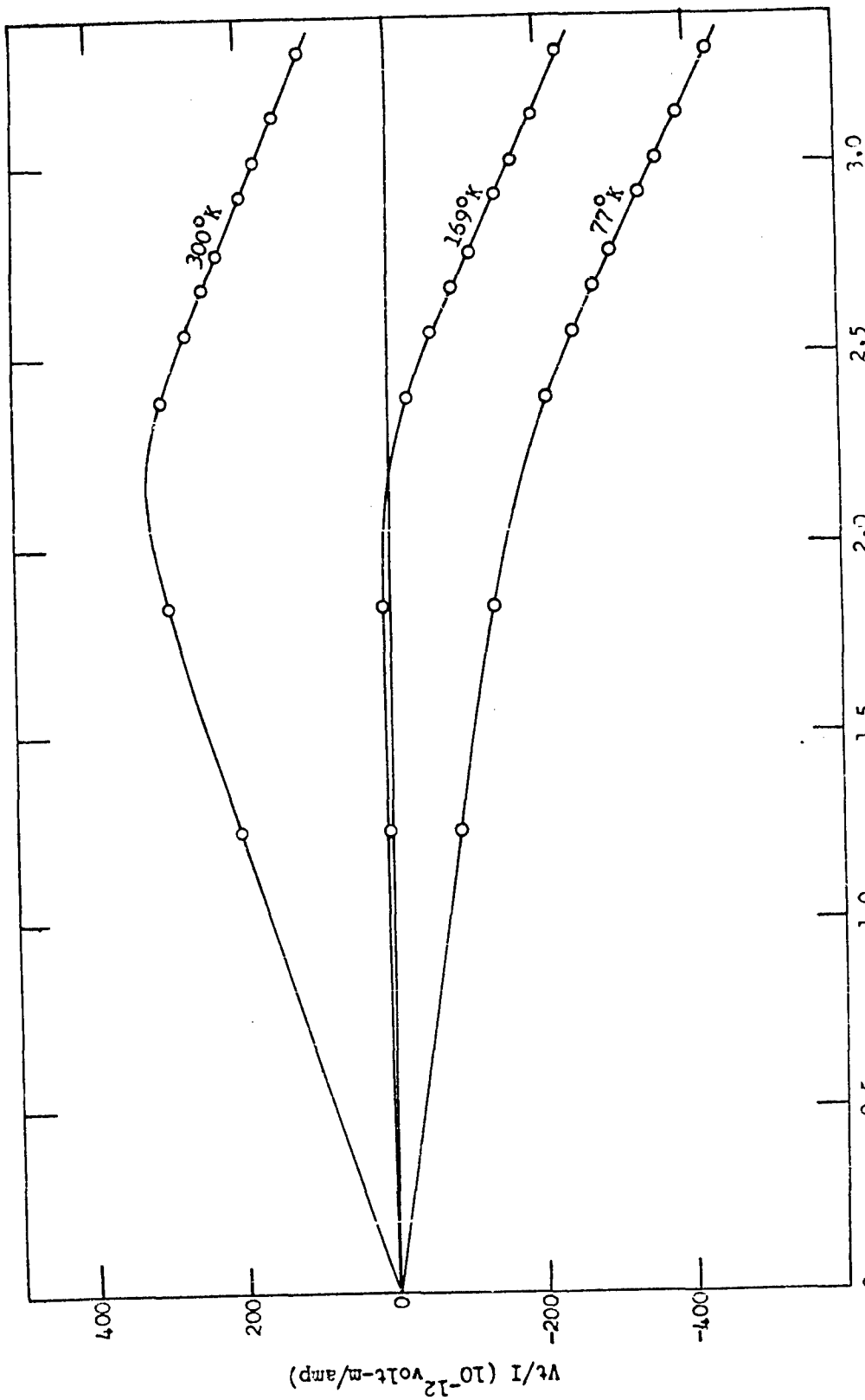

Fig. 5.7 Hall electric field per unit current density as a function of magnetic induction for 35% Cobalt - 65% Iron (annealed only).

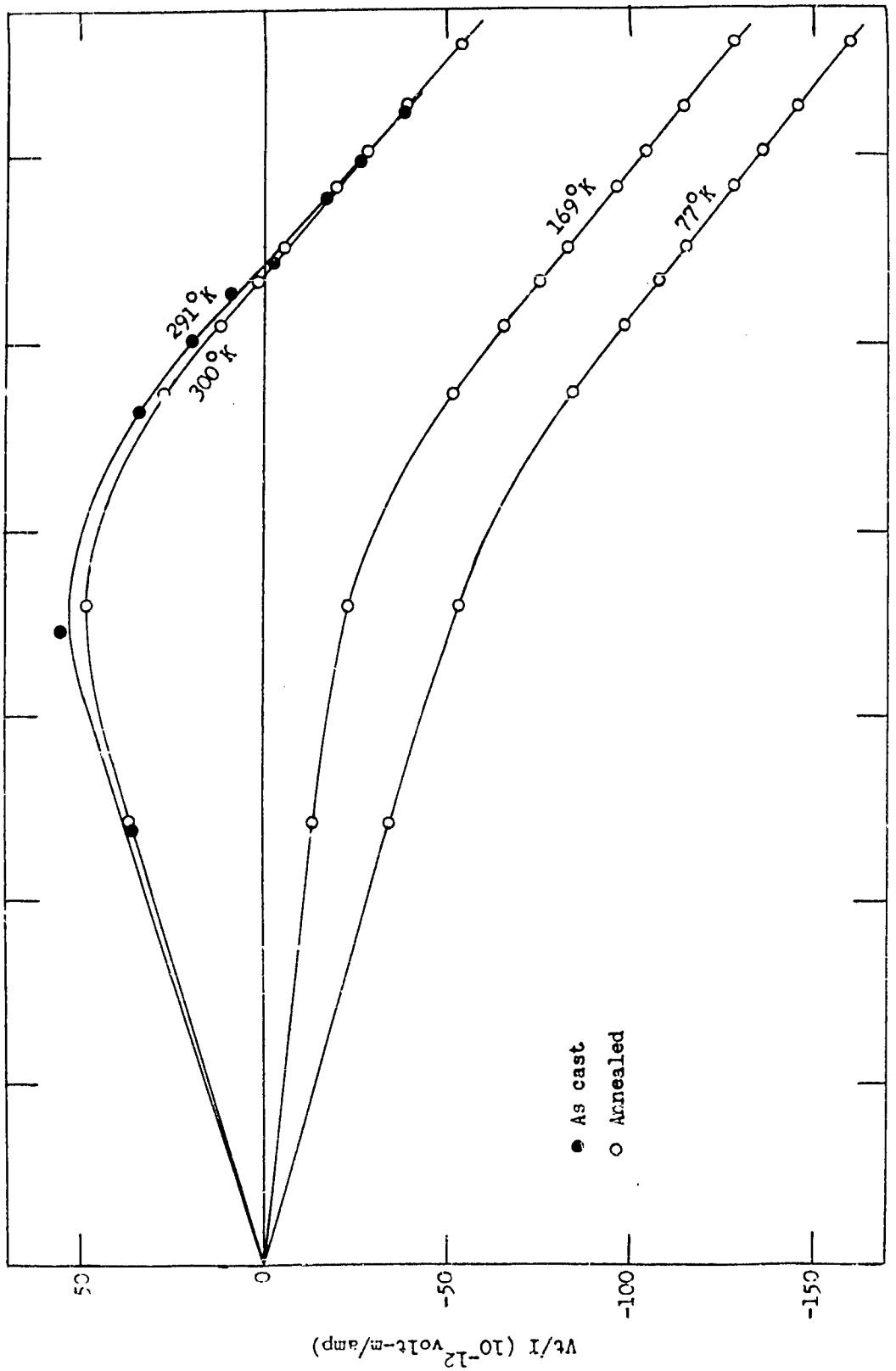

Fig. 5.3 Hall electric field per unit current density as a function of magnetic induction for 60% Cobalt - 40% Iron.

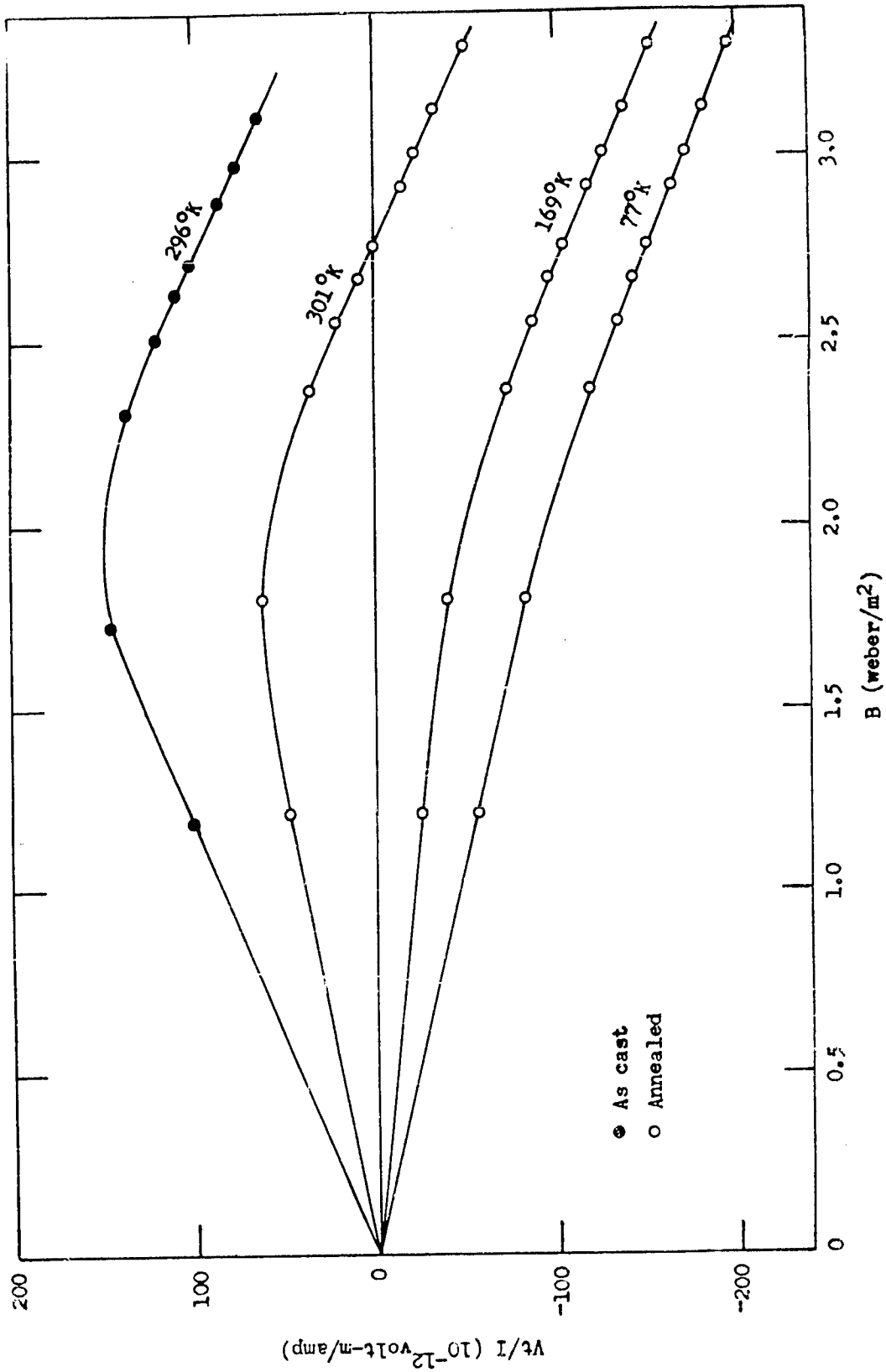

Fig. 5.9 Hall electric field per unit current density as a function of magnetic induction for 70% Cobalt - 30% Iron.

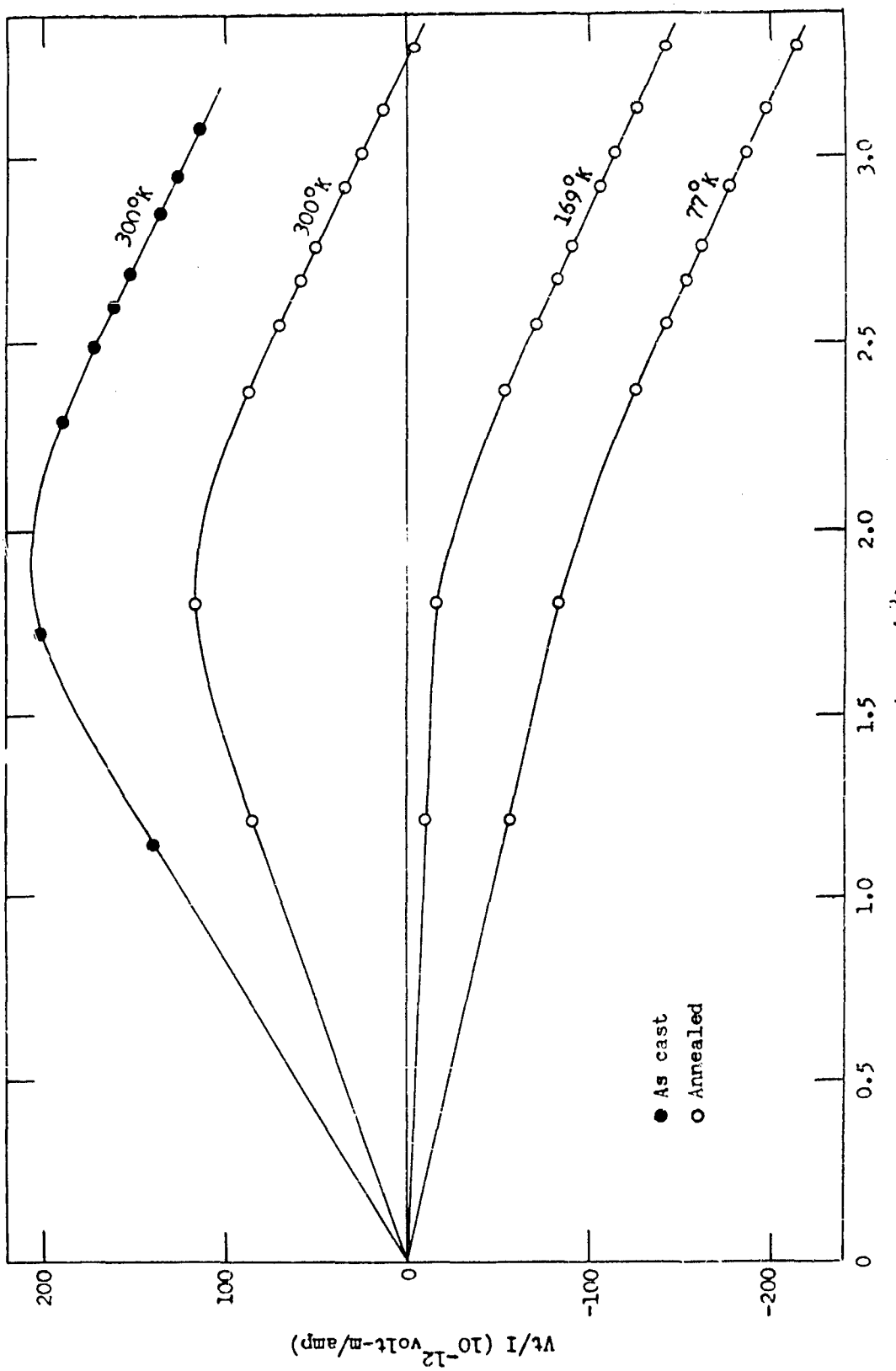

Fig. 5.10 Hall electric field per unit current density as a function of magnetic induction for 75% Cobalt - 25% Iron.

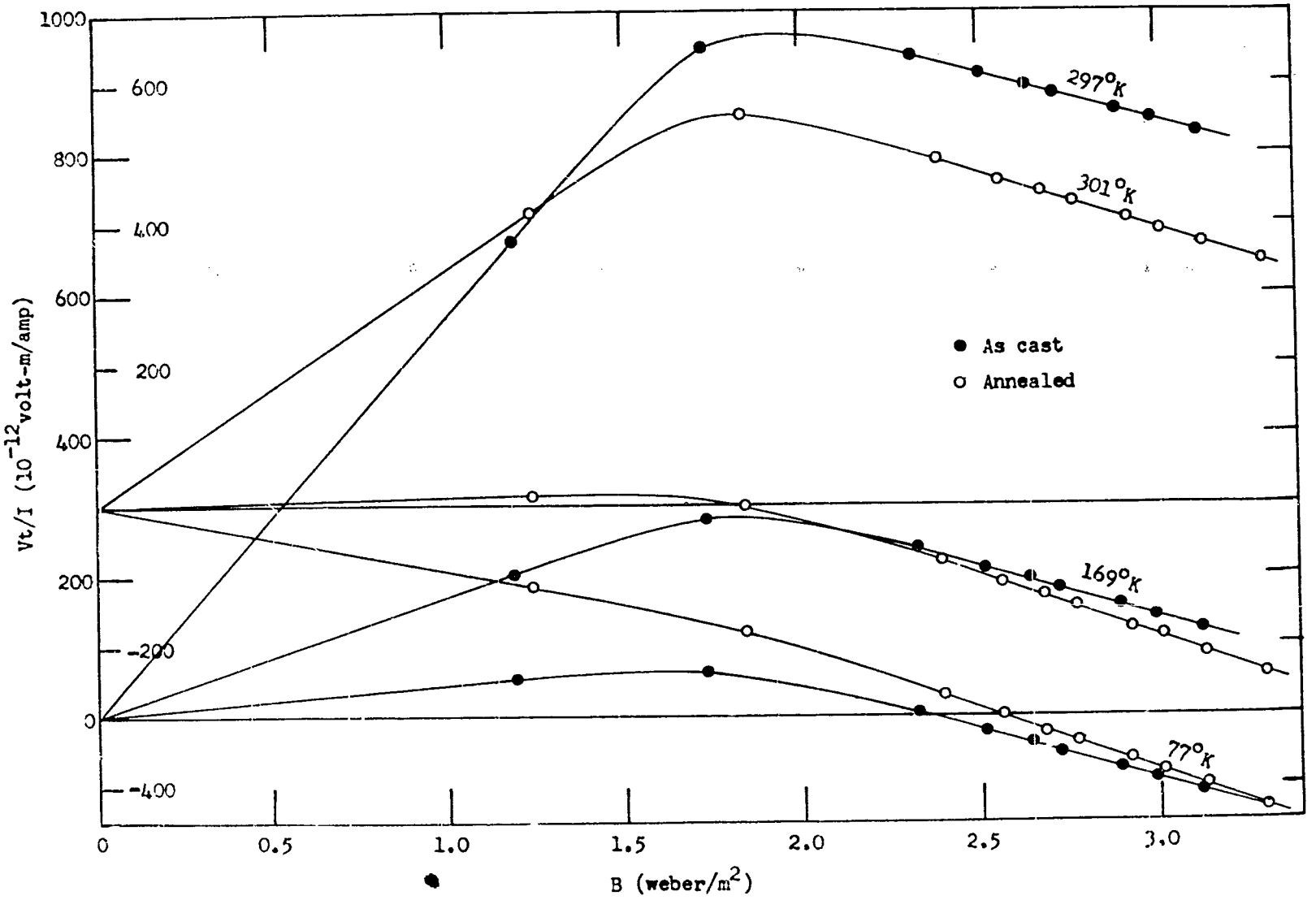

Fig. 5.11 Hall electric field per unit current density as a function of magnetic induction for 80% Cobalt - 20% Iron.

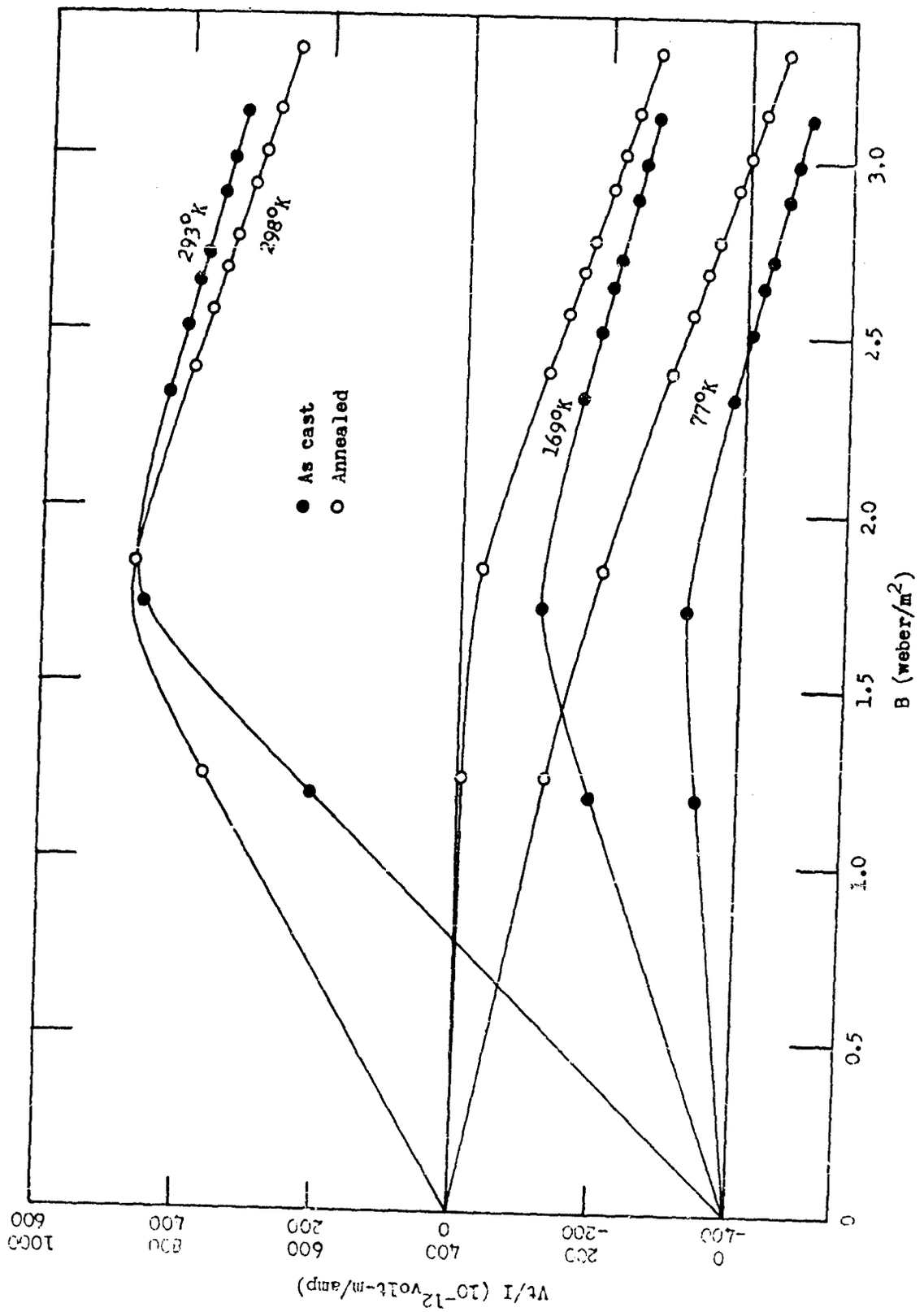

Fig. 5.12 Hall electric field per unit current density as a function of magnetic induction for 85% Cobalt - 15% Iron.

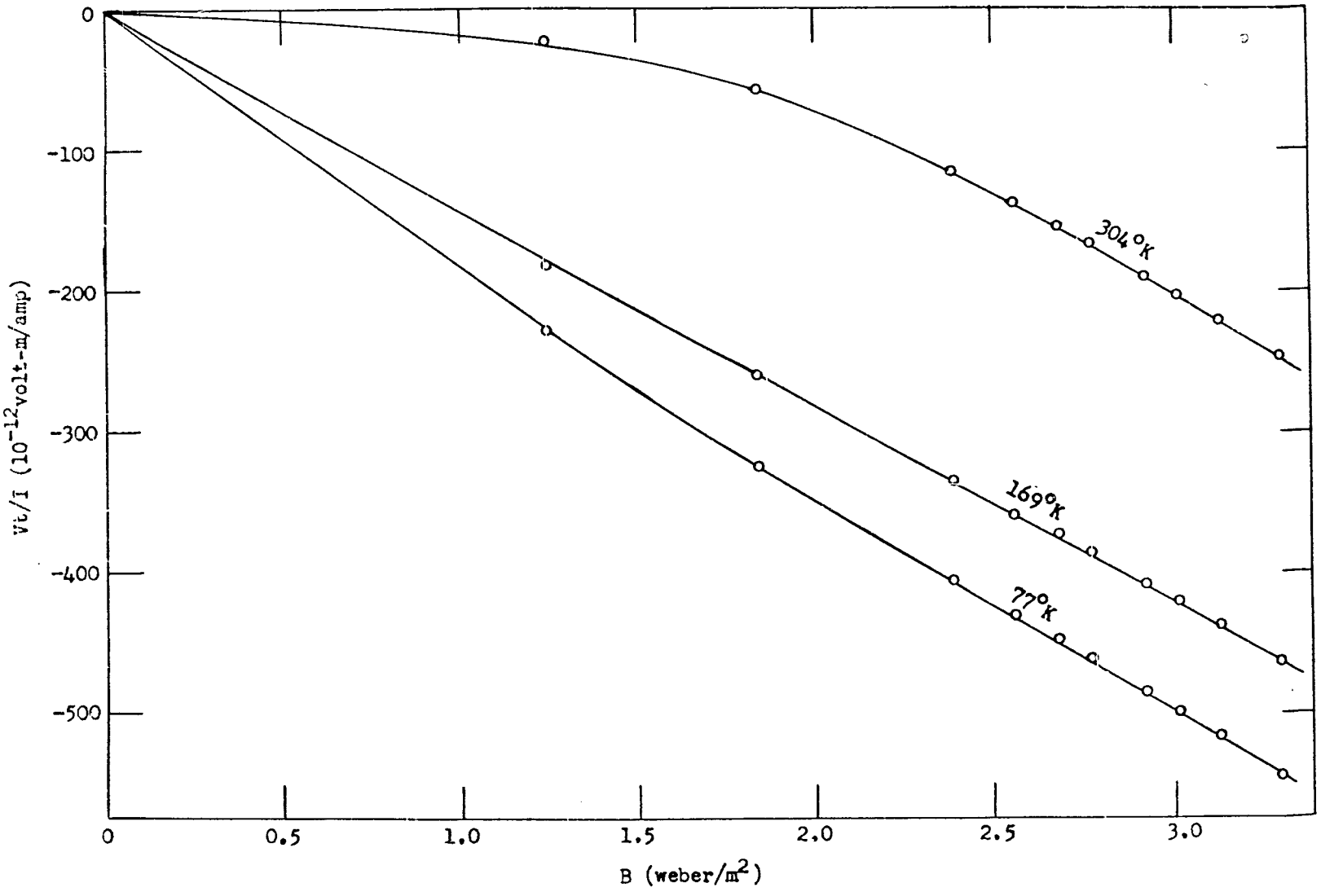

Fig. 5.13 Hall electric field per unit current density as a function of magnetic induction for cobalt (annealed only).

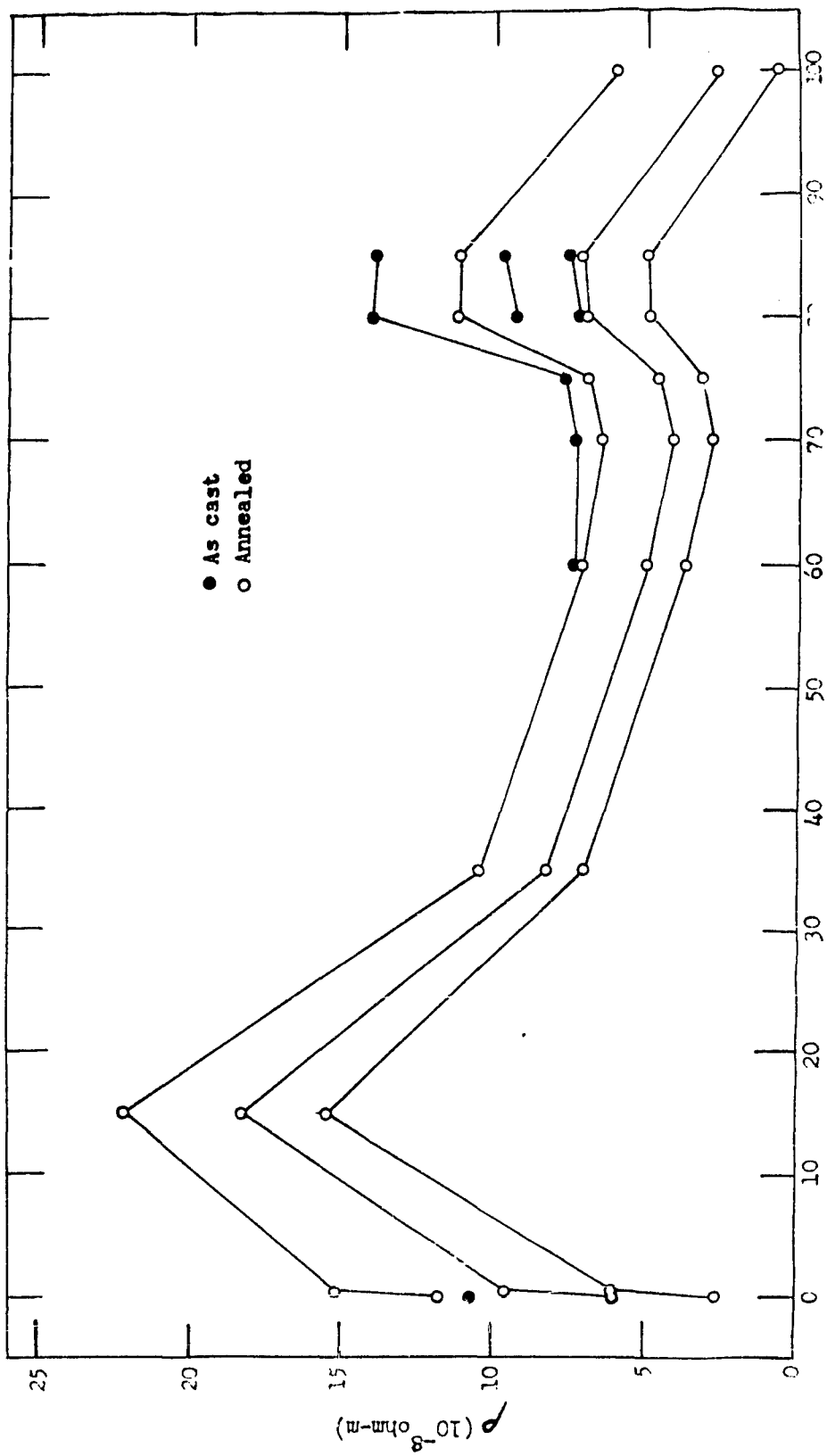

Fig. 5.14 Resistivities of the iron-cobalt alloys at 77°K, 169°K, and 293°K.

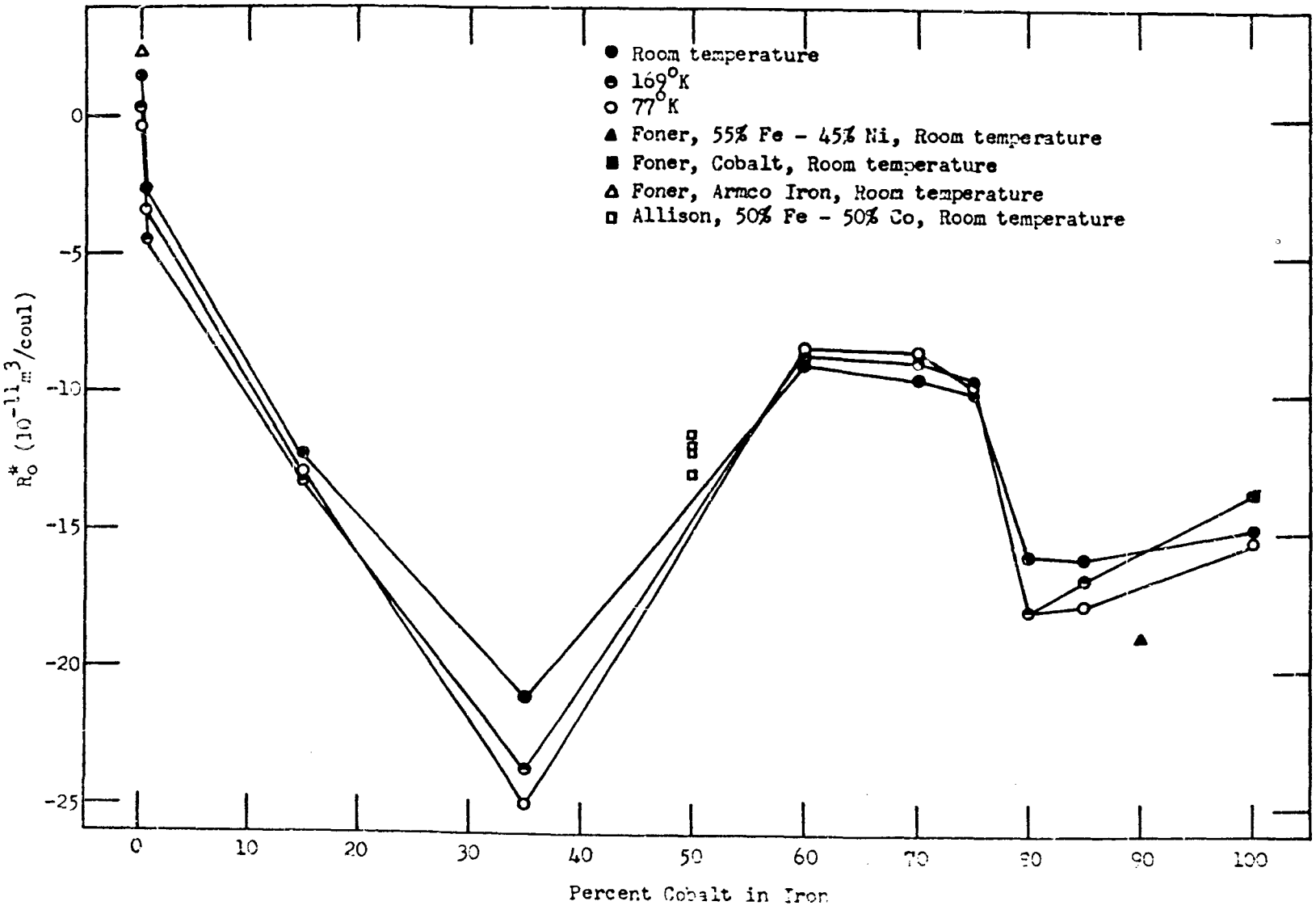

Fig. 5.15 Ordinary Hall coefficients of the iron-cobalt alloys.

Foner, Allison and Pugh[46]. The effective number of conduction electrons per atom, n^*, was calculated from the relation

$$n^* = -1/NeR_o^* = -A/dR_o^*N_o e \qquad (1.4)$$

where N_o is Avagadro's number, A is the atomic mass, e is the magnitude of the electronic charge in coulombs, and d is the density. The values obtained are shown in Fig. 5.16. The extraordinary Hall coefficient, R_1^*, was calculated using Eqs. (3.13) and (3.14) and is shown[44] in Fig. 5.17. In Figs. 5.18, 5.19, and 5.20 R_1^* is plotted as a function of the square of the resistivity.

The values[44] of R_o^*, R_1^*, n^*, and ρ are given in Tables 5.1 and 5.2.

The phase diagram[47] of the iron-cobalt system is shown in Fig. 5.21. The α and δ phases are b.c.c., the γ phase is f.c.c., the ϵ phase is h.c.p., and the α' phase is ordered b.c.c. From about 15 to 75% cobalt the alloys become non-ferromagnetic when the α to γ transformation takes place. The values of the Curie temperature, T_c, shown for this region were obtained by Forrer[48] by extrapolating the curves of magnetization versus temperature for the α phase.

46/ S. Foner, F. E. Allison, and E. M. Pugh, Phys. Rev. 109, 1129 (1958).

47/ Metals Handbook (The American Society for Metals, Cleveland, Ohio (1948).

48/ R. Forrer, J. Phys. Radium 1, 49 (1930).

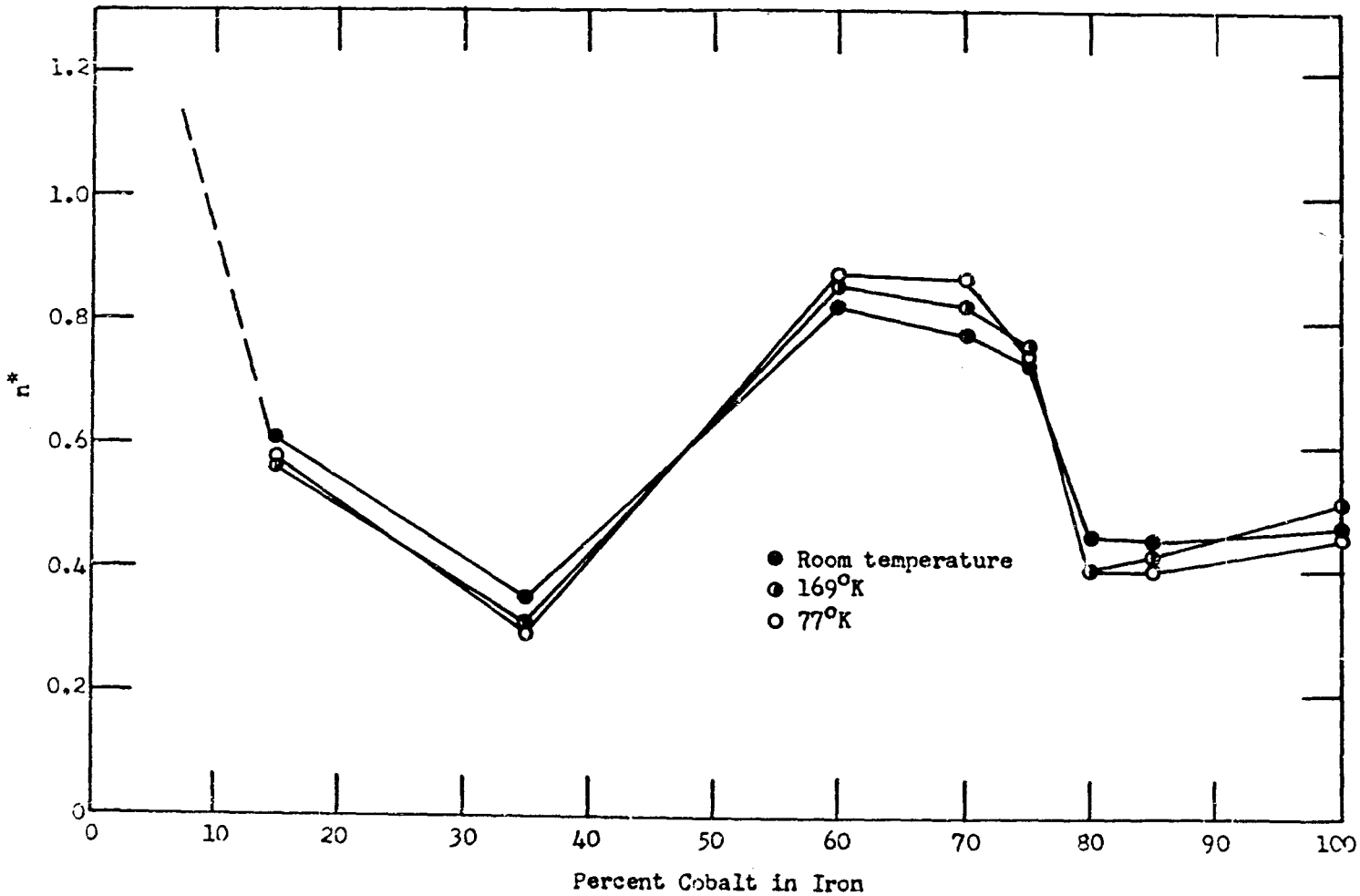

Fig. 5.16 Effective number of conduction electrons per atom in the iron-cobalt alloys.

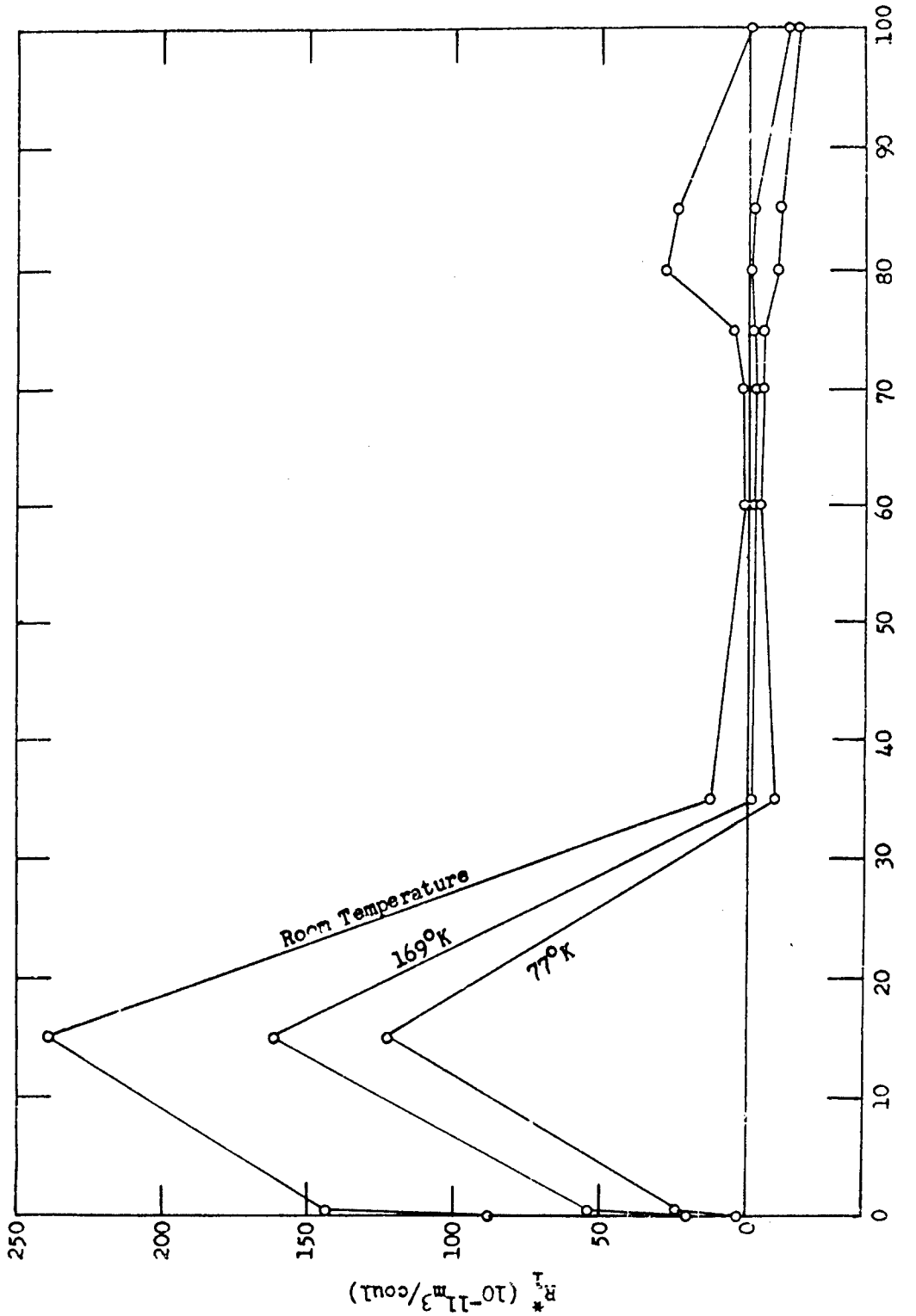

Fig. 5.17 Extraordinary Hall coefficients of the iron-cobalt alloys.

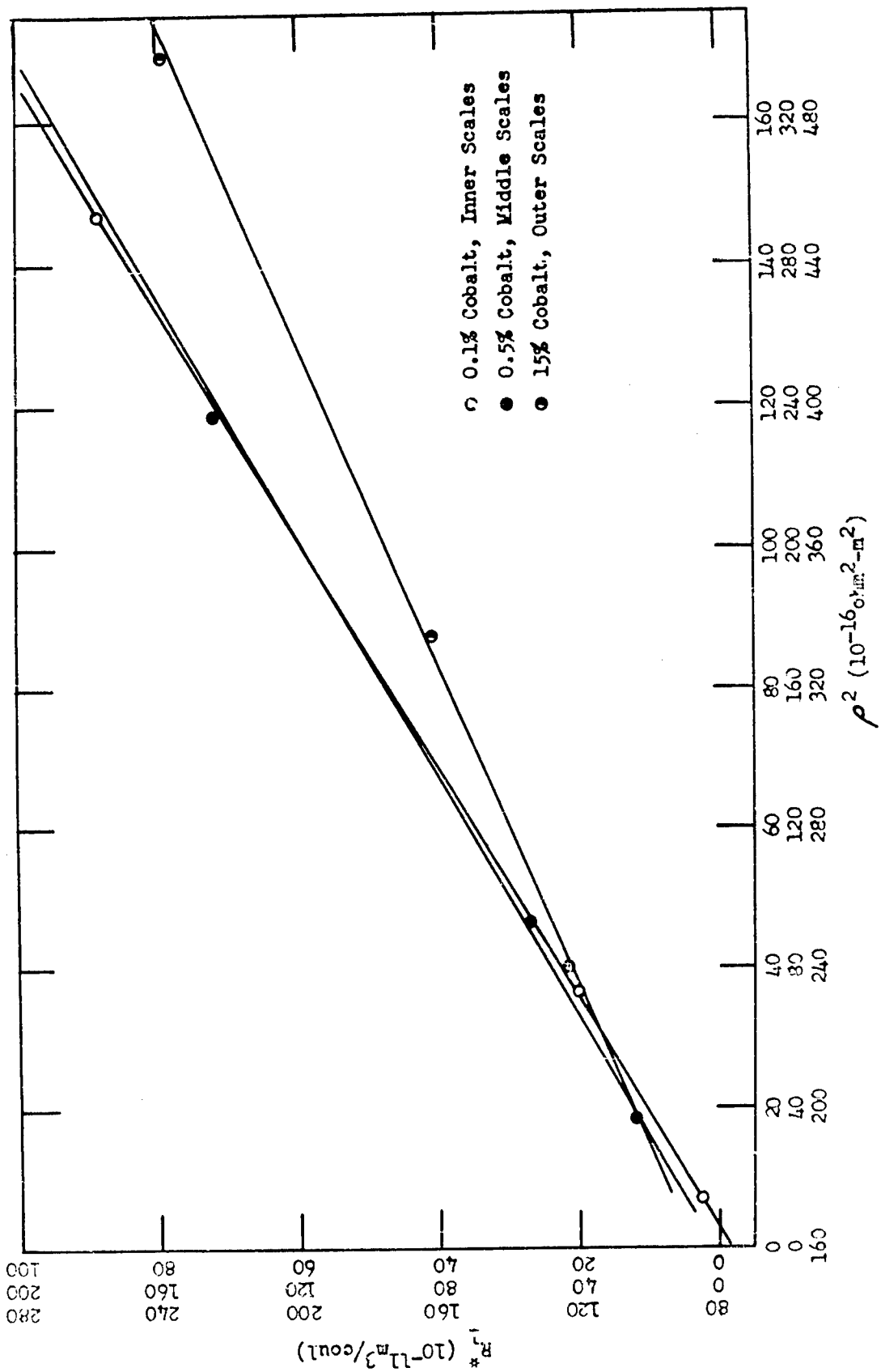

Fig. 5.18 Extraordinary Hall coefficient versus the square of the resistivity for 0.1, 0.5, and 15% Cobalt in Iron.

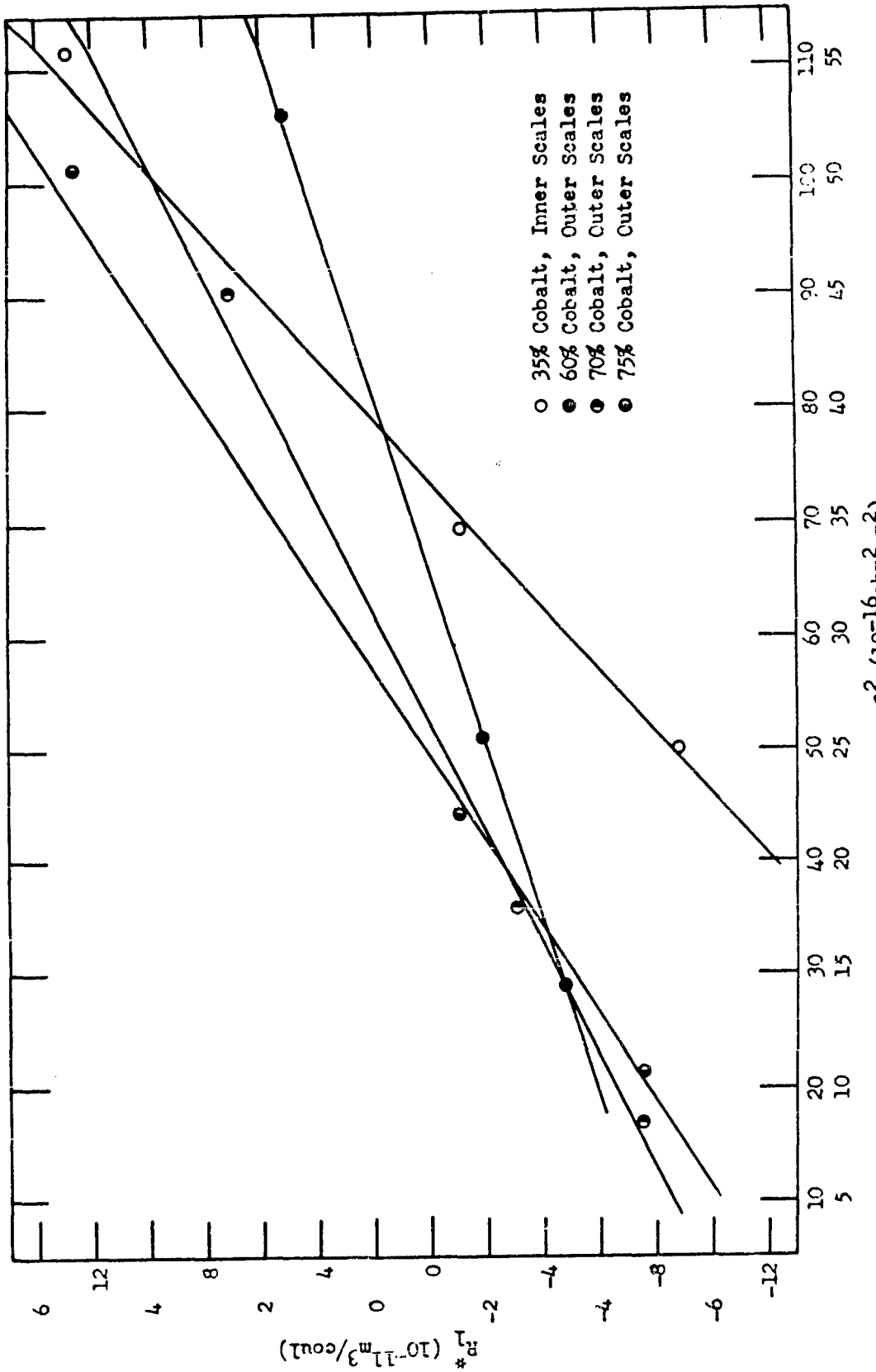

Fig. 5.19 Extraordinary Hall coefficient versus the square of the resistivity for 35, 60, 70, and 75% Cobalt in Iron.

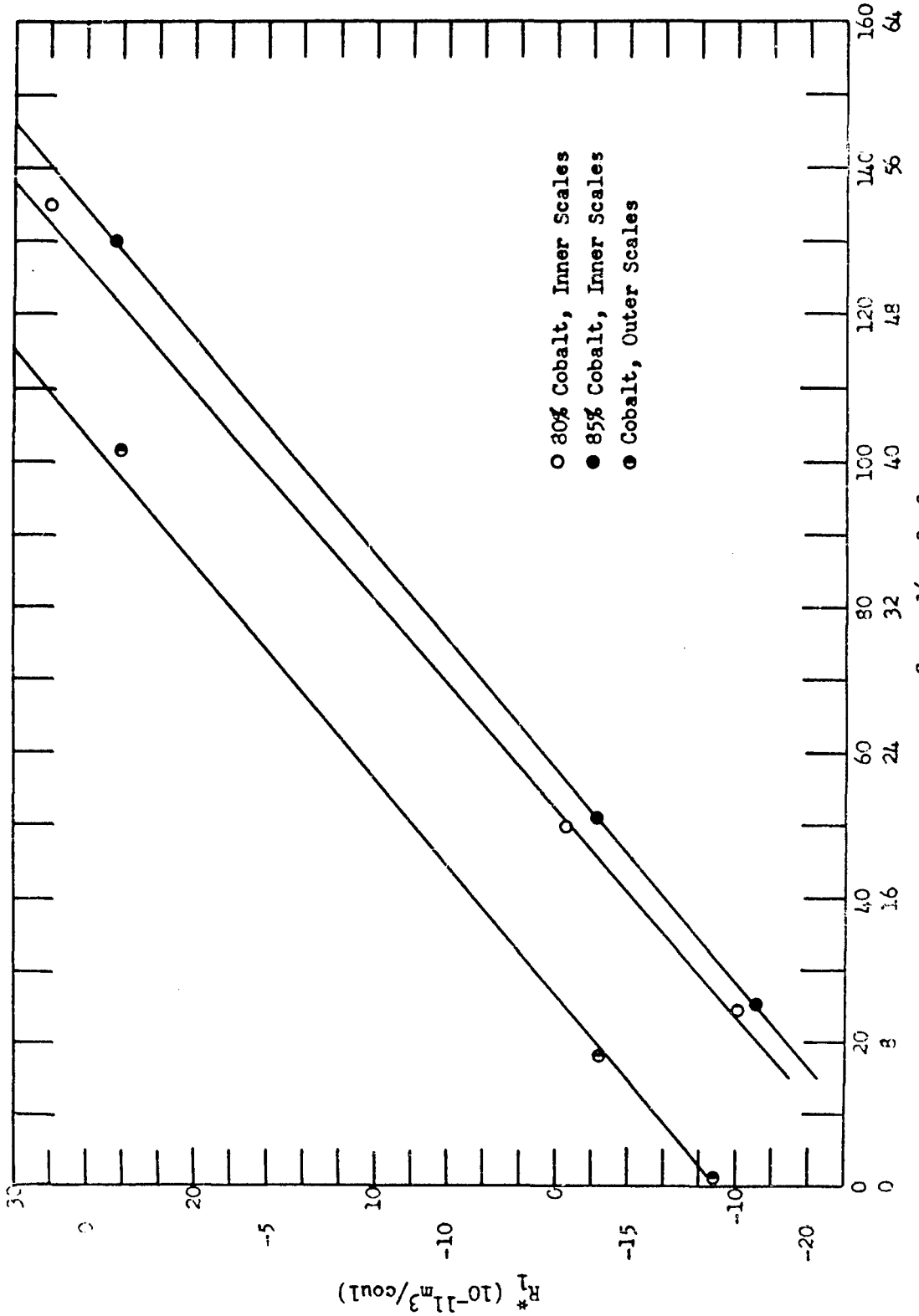

Fig. 5.20 Extraordinary Hall coefficient versus the square of the resistivity for 80, 85, and 100% Cobalt in Iron.

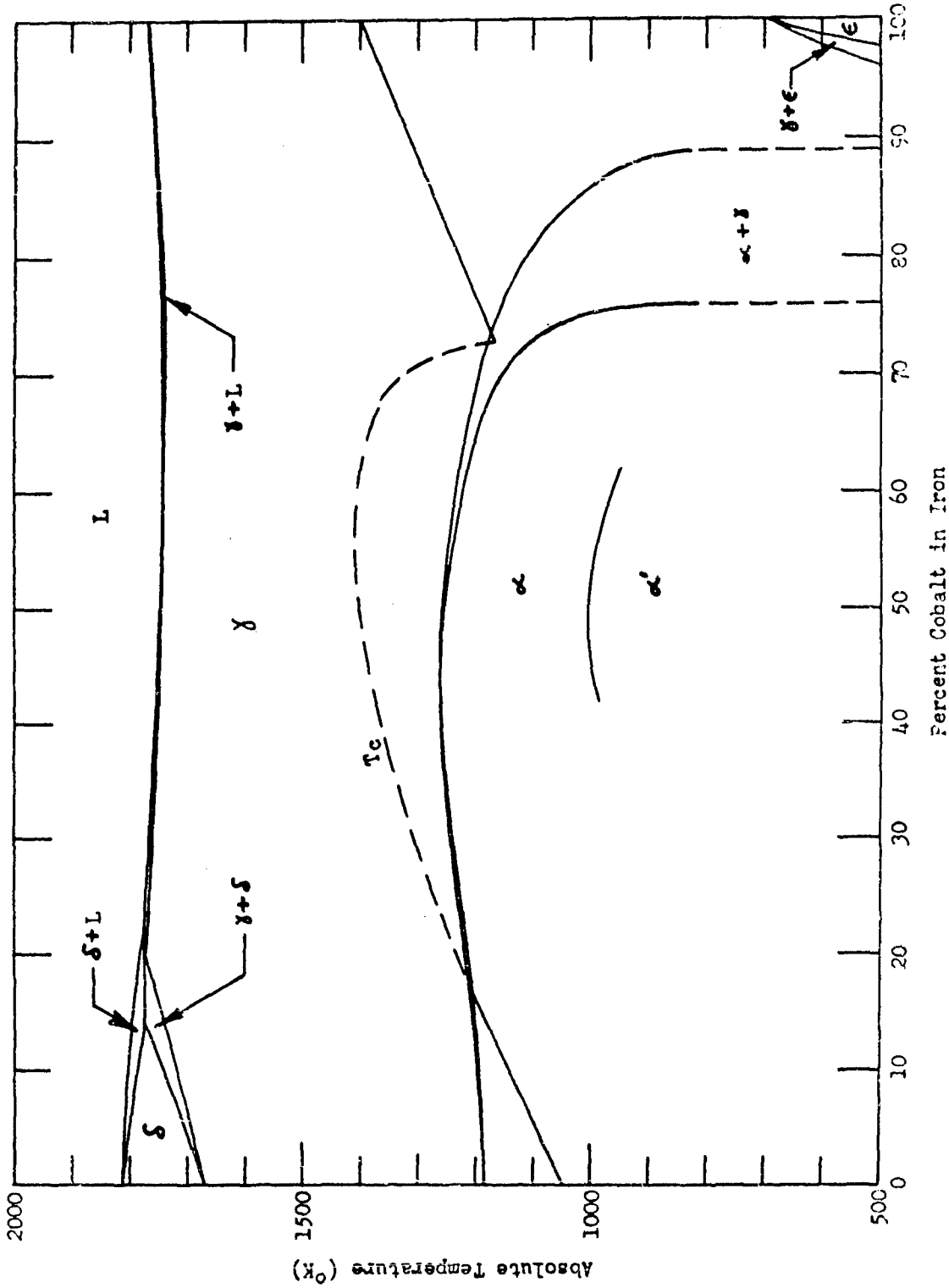

Fig. 5.21 Phase diagram for the iron-cobalt system.

Table 5.1 Summary of the Hall Coefficients, Effective Number of Conduction Electrons per Atom, and Resistivity for the As-cast Iron-cobalt Samples.

% Co	T(°K)	$-R_o^*$	n^*	R_1^*	ρ
0.1	294	-1.30	-5.714	73.39	10.81
60	291	9.59	0.767	1.82	7.35
70	296	9.34	0.778	6.86	7.52
75	300	9.88	0.732	9.65	7.85
80	77	14.20	0.505	2.46	7.24
	169	14.39	0.500	14.33	9.35
	297	13.47	0.536	49.97	14.31
85	77	12.95	0.548	3.09	7.54
	169	12.63	0.564	14.32	9.73
	293	12.79	0.559	45.58	13.93

Table 5.2 Summary of the Hall Coefficients, Effective Number of Conduction Electrons per Atom, and Resistivity for the Annealed Iron-cobalt Samples.

% Co	T(°K)	$-R_o^*$	n^*	R_1^*	ρ
0.1	77	0.35	21.0	2.50	2.66
	169	-0.32	23.0	20.11	6.05
	299	-1.44	5.21	88.46	12.17
0.5	77	3.43	2.17	23.91	6.09
	169	4.53	1.64	53.88	9.64
	297	2.66	2.81	143.9	15.41
15	77	12.91	0.575	123.1	15.52
	169	13.16	0.566	161.8	18.31
	299	12.30	0.607	238.6	22.34
35	77	24.89	0.297	-8.81	7.08
	169	23.62	0.314	-1.04	8.33
	300	21.03	0.354	12.85	10.65
60	77	8.29	0.876	-3.38	3.82
	169	8.50	0.858	-1.92	5.05
	300	8.87	0.825	1.57	7.28
70	77	8.36	0.867	-4.75	2.91
	169	8.82	0.826	-2.52	4.23
	301	9.38	0.779	2.53	6.72
75	77	9.69	0.745	-4.77	3.27
	169	9.53	0.760	-1.49	4.70
	300	9.94	0.732	5.31	7.11
80	77	17.82	0.400	-10.07	4.94
	169	17.80	0.402	- 0.55	7.05
	301	15.76	0.455	27.93	11.60
85	77	17.59	0.403	-11.05	5.03
	169	16.68	0.426	- 2.24	7.15
	298	15.90	0.448	24.28	11.41
100	77	15.26	0.453	-17.43	0.72
	169	13.62	0.510	-14.19	2.70
	304	14.85	0.469	- 1.00	6.38

6. DISCUSSION

A. Experimental Technique

Measurements were made on all samples without great difficulty at liquid nitrogen, liquid ethylene, and room temperatures. The noise level was generally quite satisfactory at all three temperatures; but occasionally the Hall potential behaved very oddly, and the data were useless. However, in the relatively few cases in which this happened, the unusual behavior could not be explained or reproduced, and other runs made later under seemingly identical conditions were quite normal.

The values of R_o^* obtained for individual runs on the same sample in the same bath differed by 1 to 5°/o, with the condition that the minimum absolute range of values was about $0.15 \times 10^{-11} m^3/coul$. For several of the samples, attempts were made to separate the Hall and Nernst effects, but no correlation could be found between R_o^* and R_1^* and the longitudinal temperature gradient per unit current (p. 15). Consequently the variations in the measured Hall constants were assumed to be random, and no corrections were made for the Nernst effect of any sample.

In order to compare the two measuring circuits (p. 40) each was used to measure the room temperature Hall effect for two samples. For the unannealed 80°/o cobalt sample R_o^* was -13.46 (25.0°C) and -13.47 (20.6°C) for the Wenner and Rubicon Thermofree Potentiometer circuits, respectively. For the unannealed 85°/o cobalt sample (without lugs) the corresponding

values of R_o^* were -12.77 (24.0°C) and -12.78 (19.6°C). The values of R_1^* were difficult to compare for the former sample due to the combination of temperatures at which runs were made; but for the latter sample the values of R_1^* at 19.6°C were 45.579 and 45.577, respectively. Obviously, the results obtained with the two circuits were in excellent agreement.

The two sample arrangements (p. 33) also were compared; the Hall effects and resistivity of the unannealed 85% cobalt sample were measured at liquid nitrogen temperature before and after lugs were machined on the sample. Measurements made with the rectangular sample and probes gave the result $R_o^* = -13.07$, $R_1^* = 3.30$, and $\rho(B = 2.99 \text{ weber/m}^2) = 7.49$. The values for the arrangement with wires spot-welded to lugs on the sample were $R_o^* = -12.83$, $R_1^* = 2.88$, and $\rho = 7.44$. These results agree within the experimental error, indicating that the geometry of the lugs is quite satisfactory.

B. Approach to Saturation

The different techniques described in Section 3C have been applied to various sets of Hall data in order to determine the role of the approach to magnetic saturation in the Hall effect.

For several of the alloys the highest fields used were more than 1 weber/m^2 above the value of M_s, and the value of a in Eq. (3.17) was small. Under these conditions the approximation given by Eq. (3.21) should apply. Accordingly this substitution

was made in the Hall equation, which was then cleared of fractions to give an observation equation linear in four unknowns involving R_o, R_1, a, and M_s. The indicated least squares calculation was made using high field data (2.37 to 3.30 weber/m^2) obtained for the 75°/o cobalt alloy in liquid nitrogen. The results were $R_o = -9.477$, $R_1 = -5.948$, $a = 0.000400$, and $M_s = 2.8343$. A plot of the data showed a good straight line relation between Vt/I and B for B greater than about 2.5 weber/m^2, and the usual calculation gave $R_o^* = -9.580$ and $R_1^* = -4.805$. On the basis of the corrections given by Eq. (3.26), the Hall coefficients are $R_o = -9.596$ and $R_1 = -4.793$, notably different from the least squares values; and M_s for this alloy is known to be only 2.16 weber/m^2 instead of the value 2.83 calculated. Since all four unknowns are so closely coupled through the least squares equations, the technique just described obviously cannot be trusted to give correct values for R_o, R_1, a, and M_s.

A possible explanation of the above result is that the approximate relation for M is not valid. However, if Eq. (3.17), the exact relation for M, is used, trial and error fitting of the data gives a similar result; the value of M_s is much too large.

An investigation of the graphical approach outlined on p. 23 leads to a better explanation of these results. The room temperature data for the 0.1°/o cobalt samples (Figs. 5.1 and 5.2) were plotted and a curve was drawn through the points for each sample. Vt/I and d(Vt/I)/dB were obtained from the curves,

and $d(Vt/I)/dB$ and $\left[(Vt/I) - Bd(Vt/I)/dB\right]$ were plotted against the functions of B and M_s indicated by Eqs. (3.22) and (3.23). Straight lines were obtained as expected, and the slopes and intercepts gave very reasonable values for R_o, R_1, and a. Figure 5.2 shows that the Hall curves had not straightened out, even at the highest fields. If they had, however, both the slope and the quantity $\left[Vt/I - Bd(Vt/I)/dB\right]$ would have become constant. Therefore, in the high field regions of the plots of these quantities, the points necessarily would have deviated from the straight line defined by the lower field points. The graphical approach thus demonstrated clearly that the straight line region of a Hall curve is a potential source of trouble in so far as the approach to magnetic saturation is concerned.

In fact, that portion of the Hall curve must be avoided in such studies, for the mere occurrence of the straight line indicates that the curvature due to the change in magnetization is masked by the experimental error. The second order term in the expansion of M about a point in the high field region gives an estimate of the deviation from the straight line due to curvature. On the basis of this estimate the Hall curves in Figs. 5.1 to 5.13 become straight about where expected for $t = 1$ mm, $I = 10$ amps, and a sensitivity of 2×10^{-9} volt. The effects of masking the curvature can be quite serious if any fitting is done in routine fashion without an actual check on the fit. For example, a function may be fitted to an experimental curve by matching a sufficient number of derivatives at a given point as well as by matching the function at a number of points.

Hence, Eqs. (3.18), (3.19), and (3.20) for a given value of B represent three equations in the unknowns R_o, R_1, and the parameters defining M(B). If the curvature, Eq. (3.20), is not well defined, obviously there are in effect only two equations in more than two unknowns. In fact, if M(B) contains two parameters, not only the second derivative but the third as well must be known or there will still be only three equations in four unknowns. It is this situation which leads to the discrepancies in the above examples. The high values for M_s and the low values for a, naturally result when the data in the straight line region are used, since this combination gives the least curvature.

Apparently the use of the Hall effect in studying the approach to magnetic saturation is quite limited. The data are useful only when the experimental errors are known to be smaller than the systematic changes anticipated, which in many cases - depending upon R_o and R_1 - means that the field as well as the potentials must be measured quite accurately. In addition, due to the geometry of the Hall samples, much higher values of H usually can be obtained by other methods.

Conversely, however, magnetic data can be useful in estimating the true Hall coefficients from the experimental values. For the iron-cobalt alloys some of the corrections to R_o^* and R_1^* given by Eq. (3.26) are surprisingly large. Because the corrections $R_o - R_o^*$ and $R_1 - R_1^*$ are both proportional to $R_1^* - R_o^*$, and because R_1^* is so large, the quantity $R_o - R_o^*$ for

the 15°/o cobalt alloy has the values -0.56, -0.72, and -1.03 at 77°K, 169°K, and room temperature, respectively. Also, because cobalt is so hard to saturate, $R_o - R_o^*$ and $R_1 - R_1^*$ are -0.60 and +0.68, respectively, at room temperature. The 0.68 correction is a large percentage of R_1^* (= - 1.00). For the 0.1 and 0.5°/o cobalt alloys $R_o - R_o^*$ is only -0.31 and -0.40, respectively, at room temperature, but these values are large compared to the small values of R_o^* (21°/o and 15°/o). Fortunately, the ordinary Hall coefficients of these four materials are such that the corrections are not important, at least at present. For the remaining alloys the corrections to both R_o^* and R_1^* are less than 1°/o.

The approach to magnetic saturation leads only to unimportant corrections in the Hall coefficients of the iron-cobalt alloys at low temperatures; but it may need to be considered in work at higher temperatures, since the corrections are proportional to $R_1^* - R_o^*$ and the magnitude of R_1^* generally increases rapidly with temperature, or in special cases in which the value of R_o^* is rather critical, as it is for the 35°/o cobalt alloy.

C. Ordinary Hall Coefficient

The plot of R_o^* as a function of temperature and composition, Fig. 5.15, has some very interesting features: the change in sign of R_o^* for the 0.1°/o cobalt alloy, the steep slope of the curve near iron, the large negative value of R_o^* for the 35°/o cobalt alloy, and the hump in the curve in the 50 to 75°/o cobalt region.

The room temperature results for cobalt and the 0.1°/o cobalt alloy agree quite well with Foner's results for cobalt and Armco iron, and the values for 50°/o cobalt and the 55°/o Fe - 45°/o Ni permalloy fall nicely on the curve. The change in sign of R_o^* with temperature near iron is not surprising since small values for the ordinary Hall coefficient can result from many different electronic configurations, and small changes can easily lead to large changes in R_o^*. Similar behavior has been observed in titanium[49], in which R_o^* ranges from about -2 at room temperature to about +3 at 1100°C.

Spikes like that at pure iron also appear at copper and nickel, as is shown in Fig. 6.1 though the peak at cobalt is much smaller and is not as sharp. The hump in the curve for the iron-cobalt alloys is unique. Comparison of Fig. 5.15 with the phase diagram, Fig. 5.21, shows that this hump appears in the region in which order-disorder transformations are observed. n^*, of course, and ρ (Figs. 5.16 and 5.14) show similar correlations with the phase diagram.

The peaks at the pure metals and the hump for the iron-cobalt alloys could be attributed to the change in scattering due to the absence of aperiodicity in the lattice. However, a close examination of the results for the 50°/o Fe - 50°/o Co samples in various states of order[46] shows that they are

---

49/ G. W. Scovil, J. Appl. Phys. 27, 1196 (1956).

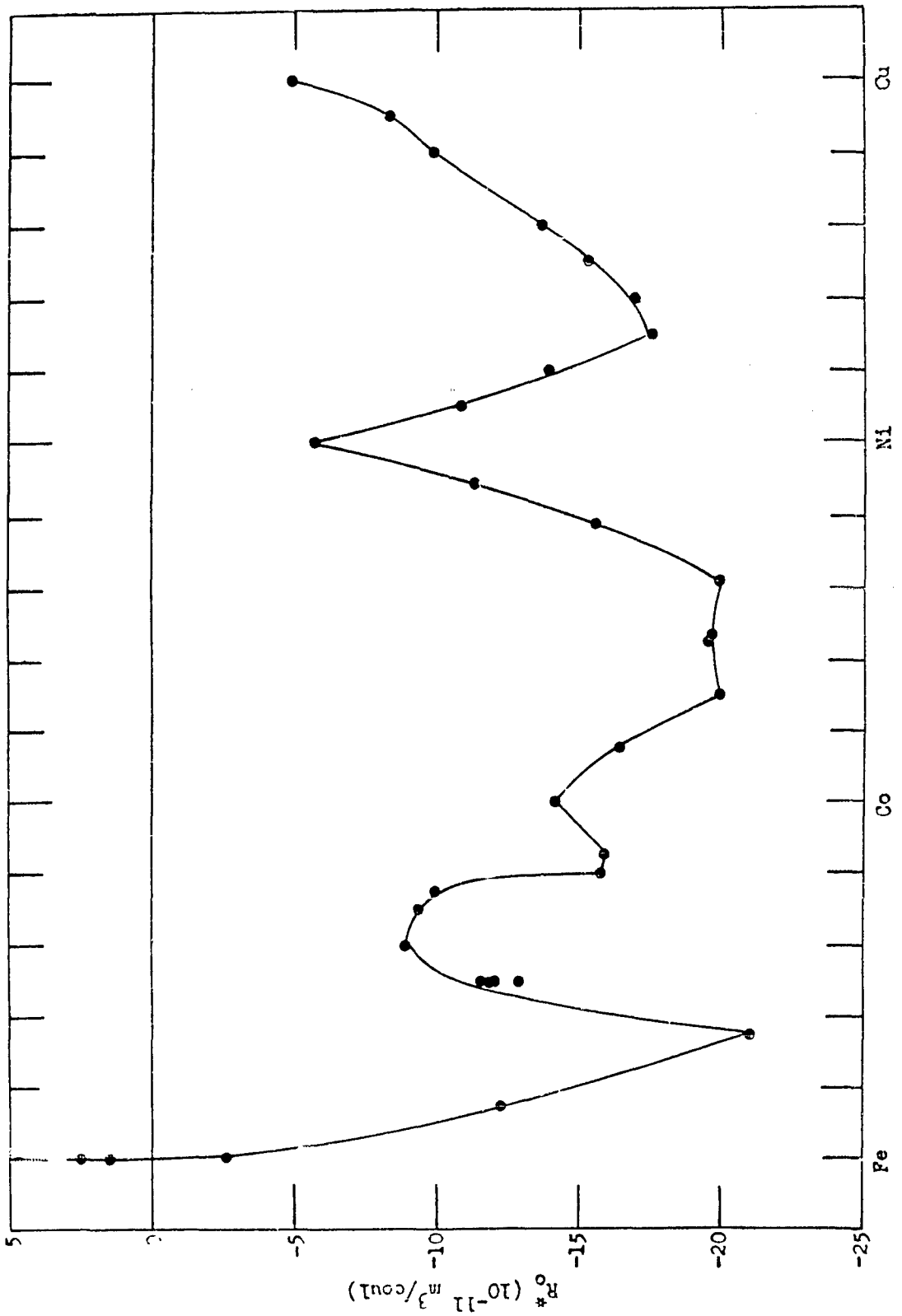

Fig. 6.1 Ordinary Hall coefficients for iron-cobalt, cobalt-nickel, and nickel-copper alloys at room temperature.

predominantly disordered. In the completely disordered alloys then, R_o^* apparently would not have the large negative value found for the 35°/o cobalt alloy, but would correspond to the lower limit of the values found for the 50°/o alloy. Thus a large part of the hump seems to result from shifts in the relative positions of the bands and, consequently, the changes in the number and mobility of the conduction electrons. Coles[50] has pointed out that a change in the scattering mechanism could easily lead to a change in R_o and, in particular, could produce the peaks in R_o^* at the pure metals. Similarly, the ordering of the lattice in the iron-cobalt alloys may contribute to the hump in R_o^* through changes in the scattering mechanism.

At 35°/o cobalt R_o^* has such a large negative value that, in terms of the band model, the explanation is practically unique. (See p. 11). If each unpaired 3d electron in this alloy contributed 1 Bohr magneton to the magnetic moment, the observed value of the magnetic moment per atom in the 35°/o cobalt alloy would require a minimum of 0.81 electron in the 4s band, while if conduction is attributed only to 4s electrons the observed Hall coefficient indicates a maximum of $2n^* = 0.58$ 4s electrons. This discrepancy can be explained by assuming that not all of the magnetic moment is due to spin but that about 10°/o is attributable to orbital motion, for the resulting decrease in the number of

---

50/ B. R. Coles, Phys. Rev. 101, 1254 (1956).

unpaired 3d electrons is sufficient to decrease the number of 4s electrons from 0.81 to 0.58. If only the two halves of the 4s band contribute to the conduction as described in Section 3A, then one half of the 3d band must be completely filled in the 35°/o cobalt alloy.

The number of 3d holes and 4s electrons were calculated from the Hall data using the number of Bohr magnetons per atom, n_o, as the number of unpaired 3d holes per atom. The results are shown in Fig. 6.2 with the curves Coles and Bitler[17] deduced from magnetic data. The values calculated from Hall data for 35°/o cobalt are those discussed in the preceding paragraph. The quantities n_d and n_s were also calculated with the number of unpaired 3d holes assumed to be 0.9 n_o to take into account the orbital contribution to the magnetic moment. These results are shown in Fig. 6.3. The conclusions are essentially unchanged; one half of the 3d band is filled for up to 20°/o iron in cobalt, then holes start to appear in both halves of the 3d band[51]. The Hall data indicate that at about 65°/o iron in cobalt the bands suddenly shift so that again one half of the 3d band is filled. As is observed near pure copper and pure nickel, very near the pure iron end of the diagram neither the magnetic data nor the Hall data lead to definite conclusions about the electronic configuration. Coles and Bitler had very few iron-rich alloys

---

51/ The actual number of holes calculated from the Hall data depends critically upon the band shape assumed.

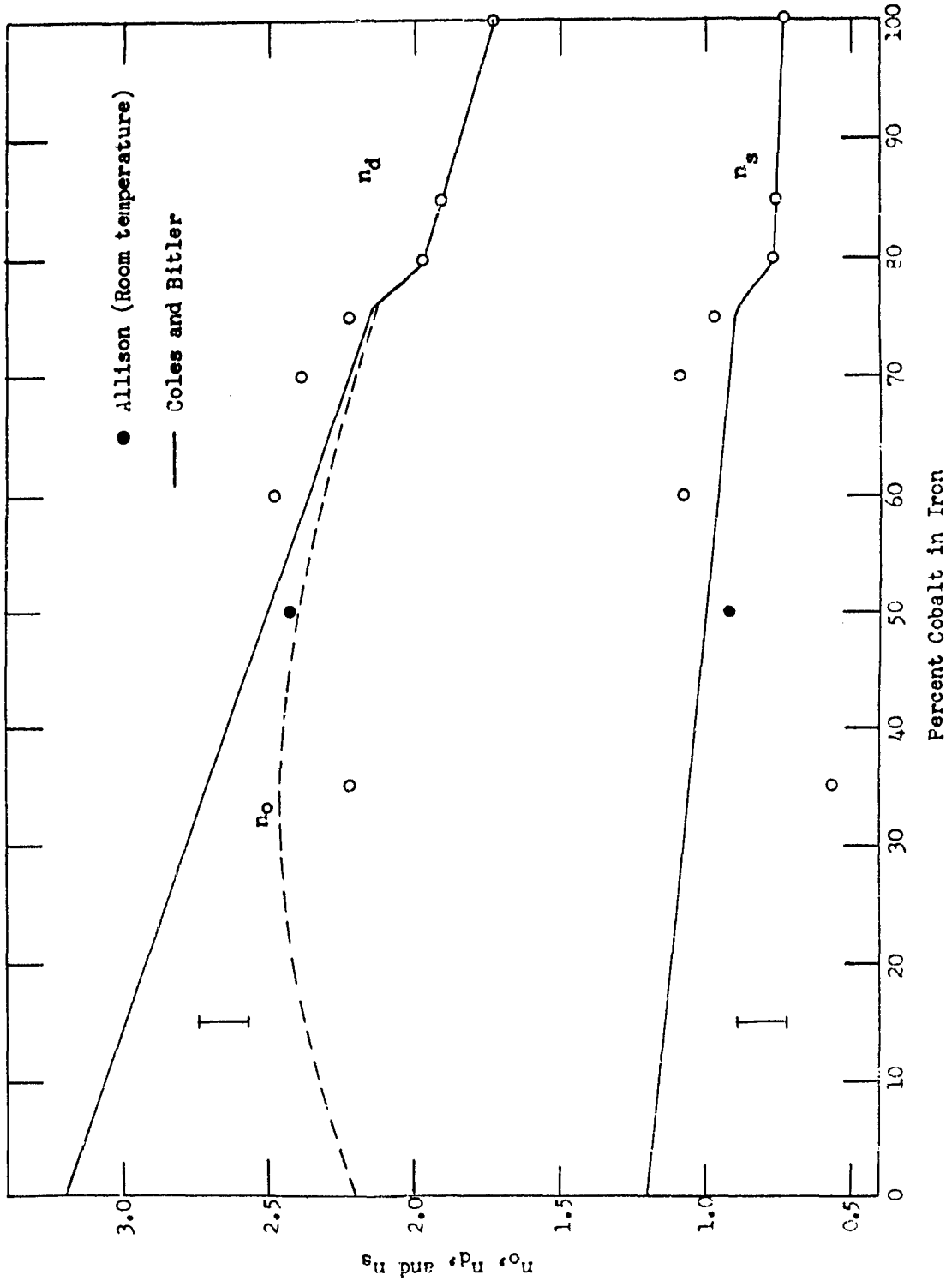

Fig. 5.2 Saturation moment in Bohr magnetons per atom (n_o), 3d-holes per atom (n_d), and 4s-electrons per atom (n_s) at absolute zero for iron-cobalt alloys.

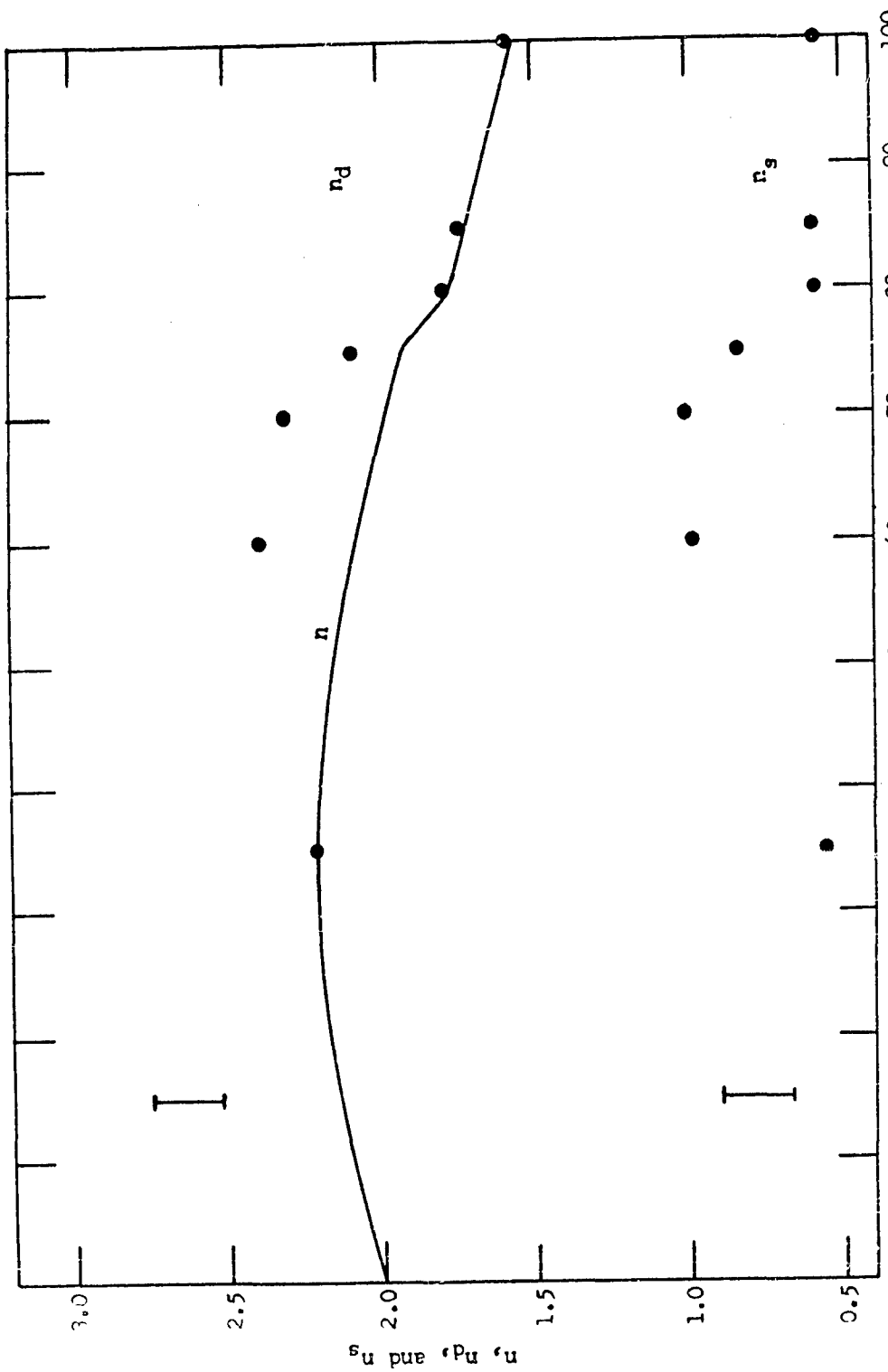

Fig. 6.3 Unpaired 3d-holes per atom (n), 3d-holes per atom (n_d), and 4s-electrons per atom (n_s) at absolute zero for iron-cobalt alloys, based on $n = 0.9n_o$.

so that their magnetic data provide little informabout about this region, and the positive value of R_o^* for iron could be due to 4s hole conduction as well as to 3d hole conduction.

D. Extraordinary Hall Coefficient

The plot of R_1^* as a function of temperature and composition for the iron-cobalt alloys, Fig. 5.17, shows an effect which has not been specifically noted before. For up to about 20°/o cobalt in iron R_1^* is apparently positive at all temperatures; but for higher cobalt content R_1^* is negative at low temperatures and increases monotonically, being positive at room temperature. This change in sign actually occurred for the 60°/o Cu - 40°/o Ni alloy measured by Cohen[8] at low temperatures, and probably would have been found for the 50°/o Cu - 50°/o Ni alloy as well if measurements had been made below 14°K. While he attributed this unusual behavior to impurities, it now seems quite reasonable on the basis of the results obtained with the iron-cobalt alloys. Figure 6.4 shows that dR_1^*/dT is positive in the iron-cobalt alloys but negative in the copper-nickel alloys. The data for the cobalt-nickel system cover only a small temperature range, but the change in sign of dR_1^*/dT apparently occurs at about 20°/o cobalt in nickel. The change in sign of R_1^* for the two copper-nickel alloys is quite consistent with the rest of the curve. Thus R_1^* can change sign if the composition is varied at fixed temperature or if the temperature is varied for a given alloy. In addition,

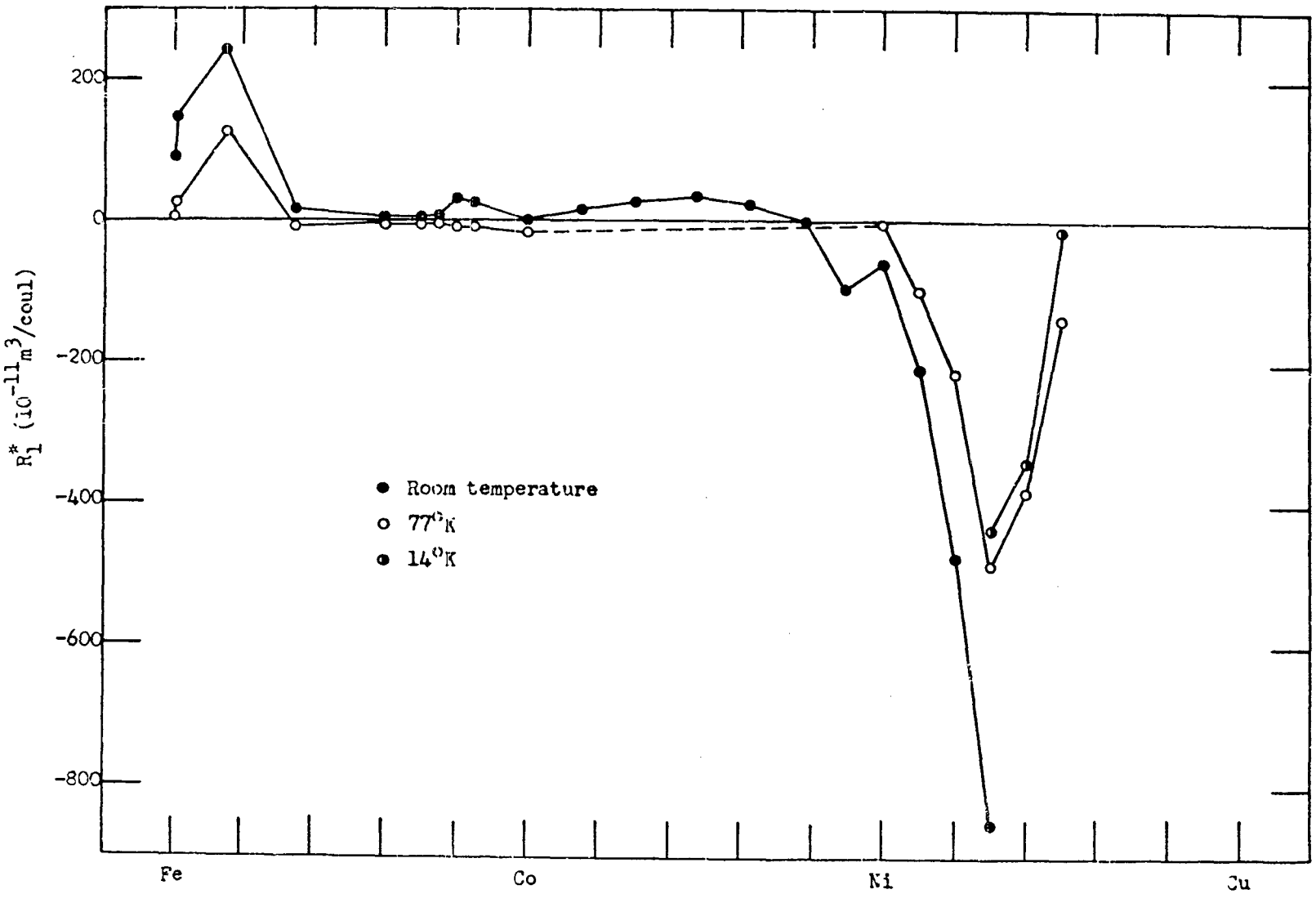

Fig. 6.4 Extraordinary Hall coefficients for iron-cobalt, cobalt-nickel, and nickel-copper alloys.

in some materials[52] R_1^* is not monotone with temperature but has a minimum value at low temperatures.

The only theories existing for R_1 have predicated either $R_1 = A\rho^2$ (Karplus and Luttinger[13]) or $R_1 - R_o = A\rho^2$ (Smit[15,16]) on the basis of a spin-orbit interaction. Plots of both log R_1 and log $(R_1 - R_o)$ versus log ρ have been made for many materials, and in many cases R_1 or $(R_1 - R_o)$ varies as ρ^n with $n \cong 2$. (See, for example, Kooi[53] and Smit[15]). For the iron-cobalt alloys, the sign change in R_1^* eliminates the form $R_1 = A\rho^n$; and, in fact, $R_1 - R_o$ also changes sign for cobalt. Many of the curves shown by Smit follow the relation $R_1 - R_o = A\rho^n$ with n ranging from 0.6 to 1.7. However, his tabulated results also include cases in which $R_1 - R_o$ changes sign.

The plots of R_1^* versus ρ^2, Figs. 5.18, 5.19, and 5.20, show that the relation $R_1^* = a + b\rho^2$ is satisfied quite well for the limited data available here. There seems to be no regular pattern in the values obtained for a; but b has a value of 0.61 at 0.1% cobalt, decreases to 0.13 at 60% cobalt, and then rises to 0.42 at cobalt. This relation has no real theoretical basis, but it has the advantage of including the other two forms commonly tested.

52/ N. S. Akulov and A. V. Cheremush'ina, Zh. eksper. teor. Fiz. 31, 152 (1956).

53/ C. Kooi, Phys. Rev. 95, 843 (1954).

7. Summary of Research on the Hall Effects of Ferromagnetic Materials and the Electronic Configurations Implied by These Data - Emerson M. Pugh

Before the beginning of this project, it was known that all of the Hall effects that had been measured in ferromagnetic materials differed by orders of magnitude with the values predicted on the theories available at that time. It had, however, been demonstrated by the author that the Hall effects that had been measured, primarily at low magnetic fields, were proportional to the magnetization rather than to the induction or the magnetizing field, as should be expected from the theory. This had suggested to the author that there must be two effects; namely, the one that had been observed but for which there was no theory, and the one that should conform to the theory but which had not been observed. The author decided to call these two effects, the "extraordinary" and "ordinary" Hall effects respectively, to distinguish them from the so-called "normal" and "abnormal" Hall effects. These latter terms were then frequently used to distinguish negative from positive Hall effects respectively.

It was believed that the "ordinary" Hall effect, that had not been observed in ferromagnetic materials, could be observed and measured at very high fields after the magnetization had become saturated. Strong steady magnetic fields together with sensitive and reliable voltage measuring techniques would be required. The author had had some success in detecting an

"ordinary" effect in nickel before he asked O.N.R. for assistance, but the available accuracy had not been sufficient to justify comparisons with theoretical predictions.

A. Discovery of the Ordinary Hall Effect

With the aid of the O.N.R. support, it was demonstrated (Technical Reports: A-1, A-2, A-4, and A-5) that there were, in fact, two Hall effects and that the "ordinary" effect, which had not been identified before, did have the proper magnitude to compare with theoretical predictions.

These researches stimulated similar work in a number of other laboratories; notably Harvard, M.I.T., Columbia, Holland, Switzerland, and Russia, in each of which the basic results were confirmed.

B. Theories for the Extraordinary Hall Effects Observed in Ferromagnetic Materials

The discovery of the ordinary Hall effect and the demonstration that it was of the right magnitude to correlate with existing theories, spotlighted the lack of theory needed to account for the extraordinary effects that had been observed for many years. N. Rostoker and the author (Technical Report A-6) suggested this was due to spin-orbit interactions with the conduction electrons. This suggestion has been developed into more formal theories by Karplus and Luttinger and by Luttinger and Kohn. These theories, especially the latter, account for the large magnitudes and the large temperature dependences that

are observed, though here the agreement between theory and experiment is as yet more qualitative than quantitative.

C. Correlation of the Ordinary Hall Effect with Band Theories

While the observations on the ordinary Hall effects (Technical Reports 1, 2, A-5, and A-7) showed that they were the right order of magnitude in the ferromagnetic elements and their alloys to agree with predictions of the simple band theory, they were often as much as a factor of two too large. The author then showed (Technical Report B-1) that all of the data on the ordinary effect, including its temperature dependence, could be correlated by assuming that, as Mott had suggested, the 3d and 4s bands each could be divided into two bands; one for the electrons with spins parallel to the field and the other for the electrons with antiparallel spins. This interpretation of the band theory made it possible to make some detailed numerical predictions for ordinary Hall effects in a number of alloys. The experiments designed to test these predictions (Technical Reports 2, B-4, B-5, and B-7), provided remarkably accurate verifications for this point of view.

D. Ordinary Hall Effects versus Total Electrons per Atom

The foregoing observations together with some additional data (Technical Reports A-6, B-2, and B-3) showed that, for many of the alloys of the first transition group of metals, the ordinary Hall effect is more characteristic of the total electrons

per atom than of the elements making up these alloys. Even in an alloy like Ni_3Mn, where Curie temperatures and the extraordinary Hall effect vary considerably with the state of order, the ordinary Hall effect is close to that of a Co-Ni alloy having the same electrons/atom.

E. Pure Elements versus Alloys

At low temperatures the alloys of the first transition group have such large ordinary Hall coefficients that the analysis is unique. The effect must be due to a small number (one half the 4s band) of conduction electrons that have considerably higher mobilities than do the other electrons. This characteristic of the ordinary Hall effect in so uniquely singling out small numbers of carriers with high mobility is of great importance. Unfortunately a small ordinary Hall effect can be explained in so many ways that it is not safe to draw conclusions when the indicated number of carriers is large; i.e. when the ordinary Hall coefficient is small.

The ordinary coefficient for all of the transition elements is small so that unique conclusions cannot be drawn concerning their electronic configurations. This leaves us in the anomalous position of being better able to understand the alloys than the pure elements.

F. Extraordinary Hall Effects in Paramagnetic Materials

Measurements on magnetic alloys at temperatures up to and above their Curie temperatures (Technical Reports 2, B-4 and B-7)

prove conclusively that very large extraordinary Hall effects are to be found in such materials when they become paramagnetic. Measurements in strongly paramagnetic alloys of the second transition group (Technical Report B-5) can be understood best in terms of an extraordinary Hall coefficient. This strongly suggests that the extraordinary Hall effect should be considered in the analysis of all Hall effects in materials having significant paramagnetism. Any material that exhibits temperature dependence of the observed Hall effect should be scrutinized for possible extraordinary effects, because no certain technique has been developed as yet for separating these two Hall effects in materials whose magnetization cannot be saturated.

8. - Bibliography of the Technical Reports Submitted on these O.N.R. Projects:

Tech. Rpt. No. 1 - "The Hall Effect of Copper Nickel Alloys," by Albert I. Schindler, June 1951 - Nonr 206(00).

Tech. Rpt. No. 2 - "Hall Effects of the Cobalt Nickel Alloys and of Armco Iron," by Simon Foner, June 30, 1952 - Nonr-206(00).

Tech. Rpt. A-1 - "On the Hall Effect in Ferromagnetics," Emerson M. Pugh, N. Rostoker, and A. Schindler, Phys. Rev. 80, 688-692 (1950).

Tech. Rpt. A-2 - "On the Hall Effect in Ferromagnetics," N. Rostoker and Emerson M. Pugh, Phys. Rev. 82, 125-126 (1951).

Tech. Rpt. A-3 - "Hall Effect and Ponderomotive Force in Simple Metals," Norman Rostoker, Am. J. of Phys, 20, 100-107 (1952).

Tech. Rpt. A-4 - "The Hall Effect in Nickel Ferrite," Simon Foner," Phys. Rev. 88, 955-956 (1952).

Tech. Rpt. A-5 - "The Hall Effect of Copper-Nickel Alloys," Albert I. Schindler and Emerson M. Pugh, Phys. Rev. 89, 295-298 (1953).

Tech. Rpt. A-6 - "Hall Effect in Ferromagnetic Materials," Emerson M. Pugh and Norman Rostoker, Rev. Mod. Phys. 25, 151-157 (1953).

Tech. Rpt. A-7 - "Hall Effects of the Cobalt Nickel Alloys and of Armco Iron," Simon Foner and Emerson M. Pugh, Phys. Rev. 91, 20-27 (1953).

Tech. Rpt. No. 1 - "Hall Effects of Copper, Nickel and the Copper Nickel Alloys at Low Temperatures," by Philip Cohen, June 30, 1955 - Nonr 760(04).

Tech. Rpt. No. 2 - "Temperature Dependence of the Hall Coefficients in Some Copper Nickel Alloys," by Floyd E. Allison, February 29, 1956 - Nonr 760(04).

Tech. Rpt. B-1 - "Band Model for Hall Effect, Magnetization, and Resistivity of Magnetic Metals," Emerson M. Pugh, Phys. Rev. 97, 647-654 (1955).

Tech. Rpt. B-2 - "Hall Effect in Permalloys," Simon Foner, Phys. Rev. 99, 1079-1081 (1955).

Tech. Rpt. B-3 - "Hall Effect and Magnetic Properties of Armco Iron," Simon Foner, Phys. Rev. 101, 1648-1652 (1956).

Tech. Rpt. B-4 - "Temperature Dependence of the Hall Coefficients in Some Copper Nickel Alloys," F. E. Allison and Emerson M. Pugh, Phys. Rev. 102, 1281-1287 (1956).

Tech. Rpt. B-5 - "Temperature Dependence of the Hall Coefficients in Some Silver Palladium Alloys," F. E. Allison and E. M. Pugh, Phys. Rev. 107, 103-105 (1957).

Tech. Rpt. B-6 - "Hall Effect in Titanium, Vanadium, Chromium, and Manganese," Simon Foner, Phys. Rev. 107, 1513-1516 (1957).

Tech. Rpt. B-7 - "Hall Effect in Ni_3Mn and Fe-Co as a Function of Order," Simon Foner, F. E. Allison and Emerson M. Pugh, Phys. Rev. 109, 1129-1133 (1958).

The following individuals have received the degree of Doctor of Philosophy in Physics as a result of their work on these projects:

Dr. A. I. Schindler

Dr. Norman Rostoker

Dr. Simon Foner

Dr. Philip Cohen

Dr. Floyd E. Allison

Dr. Frank P. Beitel, Jr.